Int J Earth Sci (Geol Rundsch) (2017) 106:1181–1203
DOI 10.1007/s00531-016-1401-5

ORIGINAL PAPER

Petrogenesis and geodynamics of plagiogranites from Central Turkey (Ekecikdağ/Aksaray): new geochemical and isotopic data for generation in an arc basin system within the northern branch of Neotethys

Serhat Köksal[1] · **Fatma Toksoy-Köksal**[2] · **M. Cemal Göncüoglu**[2]

Received: 10 April 2016 / Accepted: 10 September 2016 / Published online: 22 September 2016

Abstract In the Late Cretaceous, throughout the closure of the Neotethys Ocean, ophiolitic rocks from the İzmir–Ankara–Erzincan ocean branch were overthrusted the northern margin of the Tauride-Anatolide Platform. The ophiolitic rocks in the Ekecikdağ (Aksaray/Central Turkey) region typify the oceanic crust of the İzmir–Ankara–Erzincan branch of Neotethys. The gabbros in the area are cut by copious plagiogranite dykes, and both rock units are intruded by mafic dykes. The plagiogranites are leucocratic, fine- to medium-grained calc-alkaline rocks characterized mainly by plagioclase and quartz, with minor amounts of biotite, hornblende and clinopyroxene, and accessory phases of zircon, titanite, apatite and opaque minerals. They are tonalite and trondhjemite in composition with high SiO_2 (69.9–75.9 wt%) and exceptionally low K_2O (<0.5 wt%) contents. The plagiogranites in common with gabbros and mafic dykes show high large-ion lithophile elements/high-field strength element ratios with depletion in Nb, Ti and light rare-earth elements with respect to N-MORB. The plagiogranites together with gabbros and mafic dykes show low initial $^{87}Sr/^{86}Sr$ ratios (0.70419–0.70647), high $\varepsilon Nd_{(T)}$ (6.0–7.5) values with $^{206}Pb/^{204}Pb$ (18.199–18.581), $^{207}Pb/^{204}Pb$ (15.571–15.639) and $^{208}Pb/^{204}Pb$ (38.292–38.605) ratios indicating a depleted mantle source modified with a subduction component. They show similar isotopic characteristics to the other supra-subduction zone (SSZ) ophiolites in the Eastern Mediterranean to East Anatolian–Lesser Caucasus and Iran regions. It is suggested that the Ekecikdağ plagiogranite was generated in a short time interval from a depleted mantle source in a SSZ/fore-arc basin setting, and its nature was further modified by a subduction component during intra-oceanic subduction.

Keywords Plagiogranite · Ophiolite · Isotope · Turkey · Late Cretaceous

✉ Serhat Köksal
skoksal@metu.edu.tr

Fatma Toksoy-Köksal
ftkoksal@metu.edu.tr

M. Cemal Göncüoglu
mcgoncu@metu.edu.tr

[1] Central Laboratory, R&D Research and Training Center, Radiogenic Isotope Laboratory, Middle East Technical University, Universiteler Mah. Dumlupınar Blv. No:1, 06800 Çankaya, Ankara, Turkey

[2] Department of Geological Engineering, Middle East Technical University, Universiteler Mah. Dumlupınar Blv. No: 1, 06800 Çankaya, Ankara, Turkey

Introduction and geological setting

Silicic rocks are not widespread in oceanic environments, but they are significant because of the petrological information they carry out. Low-K silicic members of ophiolitic rocks are named generally as oceanic plagiogranites (e.g., Coleman and Peterman 1975). Related to the origin of oceanic plagiogranites, there are two main ideas (1) generation from mid-ocean ridge basalt (MORB) through extended fractional crystallization and (2) hydrous partial melting of mafic rocks, especially gabbros (e.g., Coleman and Peterman 1975; Coleman and Donato 1979; Aldiss 1981; Koepke et al. 2007; France et al. 2010; Grimes et al. 2013). The petrogenetic features of plagiogranites can provide important knowledge in determining the geodynamic nature of oceanic systems.

Turkey is located at an important area within the Tethyan realm at the conjunction of Eurasia and Gondwana (e.g., Göncüoglu et al. 1997; Göncüoglu 2014; Okay and

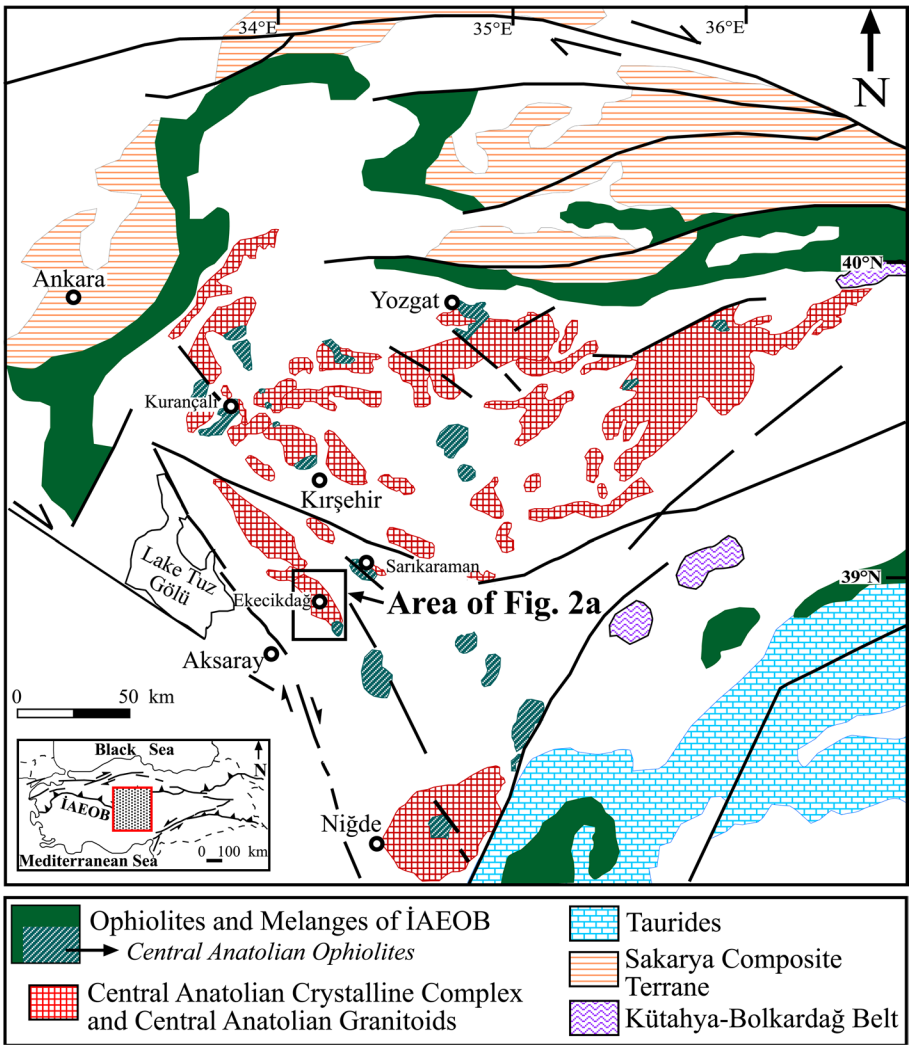

Fig. 1 Terrane map of Central Turkey (modified from Göncüoglu et al. 1997). *Dotted area* in the *inset map* shows the area of the figure. İAEOB, İzmir–Ankara–Erzincan Ophiolite Belt

Tüysüz 1999; Bozkurt and Mittwede 2001). The Alpine orogeny, which is related to the closure of the Neotethys Ocean, predominantly shaped the present geological features of Turkey and surrounding region (e.g., Moix et al. 2008; Göncüoglu et al. 2015). The Pontides at the north, a former active southern margin of Eurasia, comprise the Istranca, İstanbul and Sakarya Terranes and bounded at the south by the İzmir–Ankara–Erzincan Ophiolite (İAEO) belt (e.g., Göncüoglu et al. 1997; Moix et al. 2008). To the south of the İAEO belt in Central Turkey, the Tauride-Anatolide Platform (TAP) represents a Gondwana-derived terrane comprising the Central Anatolian Crystalline Complex (CACC) and the Menderes Massif (e.g., Göncüoglu et al. 1997, 2015). The SE Anatolian Ophiolite Belt marks the suture between the Tauride-Anatolide Terrane and the Arabian Plate (e.g., Bozkurt and Mittwede 2001; Göncüoglu et al. 2015). Ophiolitic rocks in these suture belts are of particular interest as they provide information about the vanished Tethyan oceans in the Eastern Mediterranean.

Dismembered ophiolitic rocks in Central Anatolia characterize relicts of the İAEO (Göncüoglu et al. 1991, 1997) (Fig. 1). The age of İAEO extends from the Late Carnian to the Late Cretaceous (e.g., Göncüoglu et al. 2010; Tekin et al. 2012). It was thrusted over the crustal units of the TAP in the course of the closure of Neotethys in the Late Cretaceous (e.g., Göncüoglu et al. 1997, 2015; Köksal et al. 2012, 2013). Contrariwise, there are also distinct ideas suggesting that these ultramafic and mafic assemblages in Central Anatolia are not allochthonous ophiolitic bodies but represent intrusions within the CACC (e.g., Kadıoğlu et al. 2003). Yet, it has been shown by Toksoy-Köksal et al. (2010) that especially the mafic assemblages of both intrusive and ophiolitic origin with very distinct geochemical fingerprints are present in the CACC. This distinction is partly followed by Deniz and Kadıoğlu (2016).

This research concerns mainly plagiogranites, besides mafic dykes and gabbros of the Central Anatolian Ophiolites (sensu Göncüoglu and Türeli 1993a) to the south of the Ekecikdağ (Aksaray—Turkey) being one of the type

localities in Central Anatolia (Fig. 1). In the Ekecikdağ region, as in the nearby areas, the ophiolitic rocks are thrusted over the Central Anatolian metamorphic basement and intruded by the Late Cretaceous granitoids (e.g., Toksoy-Köksal et al. 2009b).

The preliminary findings on the Ekecikdağ plagiogranites were published in Türeli et al. (1993), Göncüoglu and Türeli (1993a) and Köksal et al. (2010). The present study provides new petrological input including the isotopic data on these ophiolitic rocks from the Ekecikdağ region, to investigate the origin of plagiogranites and their relationships with the other ophiolitic rocks in the CACC and surrounding regions.

Field relations and petrography

Outcrops of the ophiolitic rocks in the study area are located at the south of the Ekecikdağ (e.g., Göncüoglu and Türeli 1993a) (Fig. 1) and include mafic and ultramafic cumulates, and layered and isotropic gabbros. Plagiogranite outcrops mainly extend as a small stock between the Göksügüzel and Bebek villages with typical occurrences on the Karaağıl Tepe and on the Kılavuz Tepe (Figs. 2, 3) within the Ekecikdağ gabbro. In the central part of the study area, where the sampling is concentrated, the screens/roof pendants of the host gabbros are found within the plagiogranites (Fig. 2b). Plagiogranites in the Ekecikdağ area are fine- to medium-grained, equigranular and generally leucocratic rocks characterized by quartz and plagioclase in hand specimen. In some samples biotite, hornblende and pyroxene contents are higher and visible up to few millimeters. Gabbros are fine- to medium-grained, dark grayish rocks mainly characterized by plagioclase, biotite and pyroxene minerals. The massive gabbros are cut by up to two-meter-thick plagiogranite dykes (Fig. 3b). Mafic dykes, which are fine-grained dark grayish- to brownish-colored rocks, cut the plagiogranites and gabbros, and chilled margins are observed at the contact zones. These dykes generally lie in the NW–SE direction and are tens of meters long and one to three meters thick (Fig. 3a).

Petrographically, the plagiogranites are medium-grained rocks with major abundance of plagioclase and quartz. Moreover, minor amounts of biotite, hornblende and clinopyroxene are present (Fig. 4a, b). Accessory amounts of zircon, titanite, apatite and opaque minerals together with

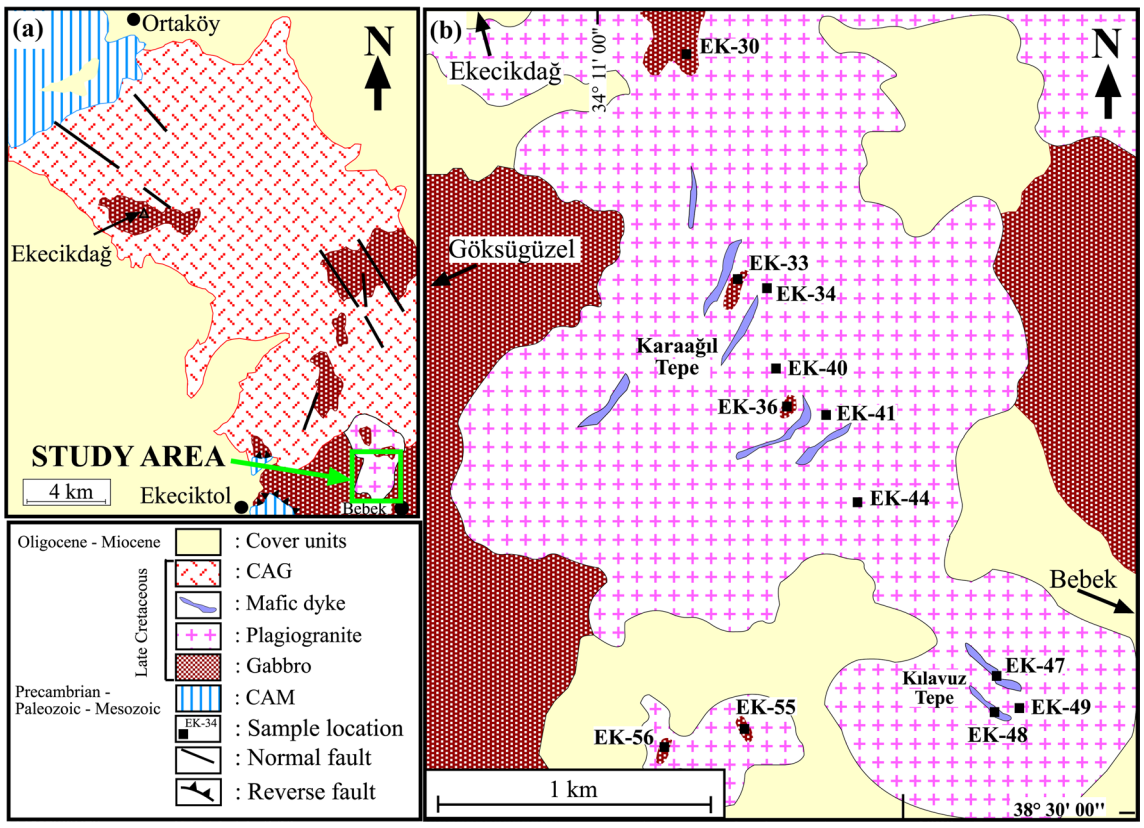

Fig. 2 **a** Geological map of the Ekecikdağ area and surrounding region (after Göncüoglu and Türeli 1993a). **b** Geological map of the study area (after Göncüoglu and Türeli 1993a). *CAG* Central Anatolian Granitoids; *CAM* Central Anatolian Metamorphics

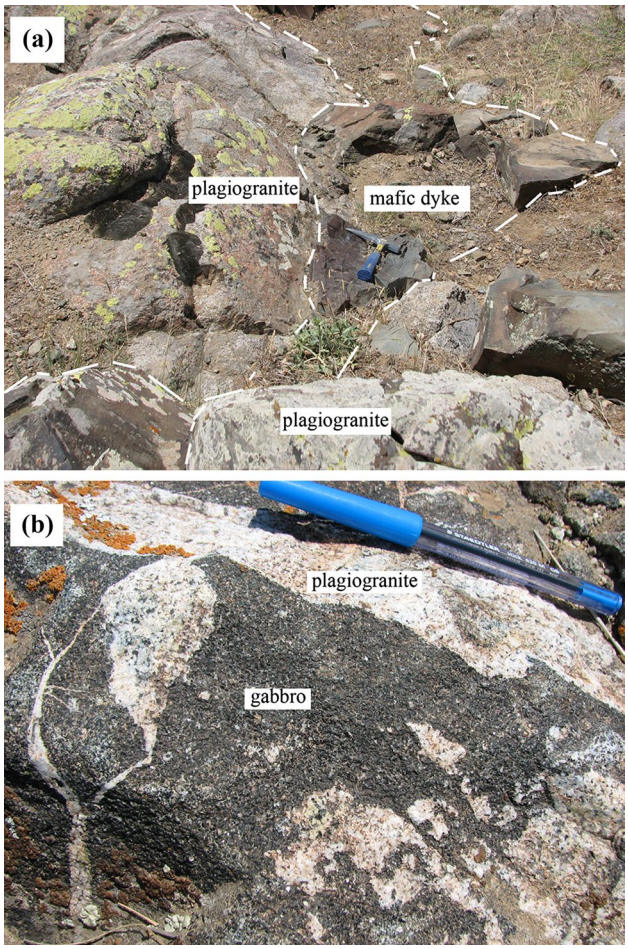

Fig. 3 Field photographs of the Ekecikdağ ophiolitic rocks, **a** mafic dyke cutting plagiogranite, **b** plagiogranite cutting gabbro

some alteration phases like chlorite, epidote and sericite are observed in the studied samples. These rocks are equigranular and characterized by hypidiomorphic to granophyric texture, with typical myrmekitic intergrowth of quartz and plagioclase (Fig. 4b). Anhedral quartz crystals with varying sizes are also found as interstitial phases among the plagioclases. Plagioclase crystals are mostly euhedral and are partly albitized at rims and along fractures. Albitization and epidotization on plagioclases along with chloritization and epidotization on pyroxenes infer sea-floor hydrothermal alteration up to low greenschist metamorphic conditions.

The gabbros are medium grained, composing essentially plagioclase and diopsidic clinopyroxene, and accessory amount of opaque and sphene. The gabbros show granular and ophitic to subophitic textures (Fig. 4c, d). Plagioclase crystals with varying sizes are euhedral to subhedral, where small plagioclase laths are found in clinopyroxenes, and fine to medium plagioclase crystals are distributed through mafic crystals. Subhedral to anhedral clinopyroxene crystals enclose plagioclases. The textural features infer that the crystallization order of the gabbro is plagioclase → plagioclase + clinopyroxene. Thus, two generation of plagioclase is likely to be present in the gabbro samples.

The mafic dykes are fine-grained rocks containing euhedral to subhedral plagioclase laths, uralitic hornblende displaying poikilitic texture having clinopyroxene relicts with rare quartz and accessory opaque minerals (Fig. 4e, f). Ferromagnesian minerals are interstitially distributed among the plagioclase laths. Actinolitic replacement of the hornblende as a product of alteration is common in the mafic dykes.

Analytical methods

Geochemical analyses of the major, trace and rare-earth elements (REE) (Tables 1, 2, 3, 4) and isotope analyses from five representative whole-rock samples from plagiogranites were performed to determine the petrogenetic features of the plagiogranites in the study area. For comparison, elemental and isotopic analyses of whole-rock samples from gabbros and mafic dyke units were also done. Elemental concentrations were determined subsequent to lithium metaborate/tetraborate fusion and dilute nitric acid digestion by inductively coupled plasma atomic emission spectrometer (ICP-OES) for major elements and inductively coupled plasma mass spectrometer (ICP-MS) for trace and rare-earth elements at ACME Analytical Laboratories Ltd. (Canada). Results of the STD SO-18 (in-house reference material of ACME Analytical Laboratories Ltd.) are also reported in Tables 1, 2 and 3.

Strontium, Nd and Pb isotope analyses were performed at the Radiogenic Isotope Laboratory of Central Laboratory, Middle East Technical University, Ankara, Turkey (Tables 5, 6). Chemical treatment and column chemistry were performed in 100-class clean laboratory with ultrapure chemical agents. Powdered rock samples (approximately 120 mg) were leached with 4 ml of 52 % HF for 4 days on the hot plate (>100 °C). These samples were dried and dissolved overnight in 4 ml 6 N HCl on the hot plate. Afterward samples were dried, and one-third of the samples were separated and dissolved in 2 N HCl for Pb chromatography, and remaining parts were dissolved in 2.5 N HCl for Sr and Nd chromatography.

Strontium was separated from other elements in 2 ml volume BioRad AG50 W-X8 (100–200 mesh) resin in Teflon columns in a 2.5 N HCl medium. After separation of Sr, excessive Ba was removed by using 2.5 N HNO_3. Subsequently REE fraction was enriched with 6 N HCl in these columns. Neodymium was separated from REE fraction in 2 ml HDEHP (bis-ethyexyl phosphate)-coated biobeads (BioRad) resin by using 0.22 N HCl in Teflon columns. Strontium was loaded on single Re filaments with

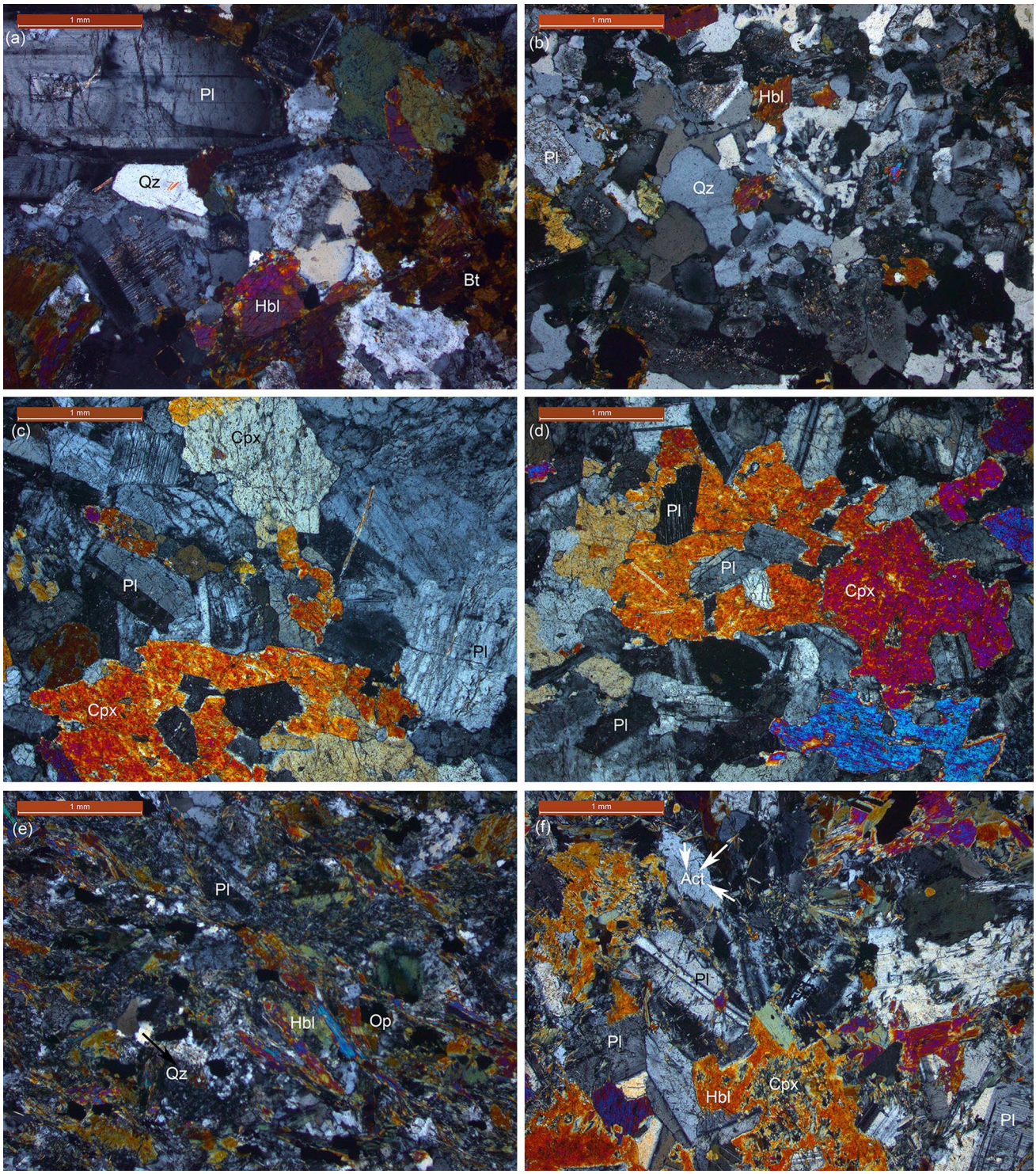

Fig. 4 Petrographic microphotographs of the Ekecikdağ ophiolitic rocks (**a**) and (**b**) plagiogranites, (**c**) and (**d**) gabbro, (**e**) and (**f**) mafic dyke. *Pl* plagioclase; *Qz* quartz; *Bt* biotite; *Hbl* hornblende; *Cpx* clinopyroxene; *Op* opaque; *Act* actinolite

0.005 N H_3PO_4 and Ta activator to improve efficiency. Neodymium, on the other hand, was loaded on double filaments with 0.005 N H_3PO_4. $^{87}Sr/^{86}Sr$ ratios are normalized with $^{86}Sr/^{88}Sr = 0.1194$, and $^{143}Nd/^{144}Nd$ ratios were normalized with $^{146}Nd/^{144}Nd = 0.7219$. During the analyses NIST SRM 987 and La Jolla Nd standards were measured as $^{87}Sr/^{86}Sr = 0.710258 \pm 10$ ($n = 2$) and $^{143}Nd/^{144}Nd = 0.511847 \pm 5$ ($n = 2$), respectively, and no

Table 1 Major element compositions of the rock units in the study area

	SiO_2 %	Al_2O_3 %	Fe_2O_3 %	MgO %	CaO %	Na_2O %	K_2O %	TiO_2 %	P_2O_5 %	MnO %	Cr_2O_3 %	LOI %	Total %
Plagiogranites													
EK-34	75.92	12.81	2.51	0.34	2.46	4.22	0.18	0.16	0.026	0.11	0.024	1.2	99.96
EK-40	71.84	14.29	3.28	0.60	4.11	3.81	0.25	0.30	0.070	0.08	0.048	1.3	99.98
EK-41	71.40	14.07	4.04	0.82	4.43	3.46	0.49	0.34	0.070	0.09	0.046	0.7	99.96
EK-44	69.87	13.83	5.17	1.13	4.45	3.73	0.40	0.44	0.072	0.10	0.051	0.7	99.95
EK-49	71.53	13.55	4.11	0.92	3.91	3.38	0.41	0.33	0.062	0.09	0.053	1.6	99.94
Gabbros													
EK-30	50.71	17.11	9.67	8.13	11.60	1.23	0.14	0.37	0.037	0.17	0.023	0.6	99.80
EK-33	49.64	19.70	2.48	5.72	18.29	2.11	0.10	0.56	0.071	0.05	0.031	1.1	99.85
EK-36	49.85	17.67	2.96	6.83	18.39	1.93	0.05	0.35	0.015	0.06	0.030	1.7	99.83
EK-55	52.80	15.68	10.06	6.71	11.50	1.38	0.09	0.70	0.079	0.14	0.039	0.6	99.79
EK-56	53.12	15.46	8.68	7.77	11.82	1.09	0.16	0.34	0.027	0.17	0.041	1.1	99.79
Mafic dykes													
EK-47	52.13	16.63	12.14	5.56	9.66	2.00	0.10	0.54	0.040	0.19	0.016	0.8	99.81
EK-48	48.94	14.99	10.45	9.94	12.32	1.23	0.10	0.74	0.065	0.17	0.077	0.7	99.74
Standard													
STD SO-18	58.10	14.14	7.62	3.33	6.38	3.69	2.15	0.69	0.802	0.39	0.549	1.9	99.74

Table 2 Some trace element compositions of the rock units in the study area

	Ba ppm	Cs ppm	Ga ppm	Hf ppm	Nb ppm	Rb ppm	Sr ppm	Th ppm	U ppm	V ppm	Zr ppm	Y ppm	Pb ppm	Zn ppm	Cu ppm	Ni ppm	Sc ppm	Mo ppm	Co ppm
Plagiogranites																			
EK-34	76	0.3	12.0	3.2	0.9	2.3	102.3	0.6	0.3	10	90.0	37.9	0.9	63	7.5	4.8	9	2.2	2.0
EK-40	52	1.1	13.0	2.0	0.7	9.1	103.4	0.2	0.2	24	53.9	24.9	0.6	22	6.0	7.5	11	5.3	3.9
EK-41	58	0.6	12.5	1.7	0.7	10.5	80.6	0.2	0.1	40	45.2	28.4	0.6	30	3.5	5.9	16	5.1	5.4
EK-44	53	0.3	13.4	1.5	0.7	7.0	77.5	0.2	0.1	83	34.5	39.2	0.9	24	7.5	7.2	23	5.4	8.4
EK-49	66	1.4	13.2	2.2	0.7	13.8	84.1	0.3	0.2	44	51.9	36.3	1.0	25	6.6	8.5	17	6.1	6.2
Gabbros																			
EK-30	29	0.6	12.2	0.4	0.2	3.5	65.9	0.2	0.1	310	9.4	9.7	0.9	7	35.2	13.3	46	1.7	42.2
EK-33	12	0.4	11.6	1.7	0.6	2.0	241.1	0.2	0.1	233	44.7	25.5	1.2	4	7.7	4.6	49	3.0	9.0
EK-36	14	0.3	10.9	0.8	0.3	1.8	151.1	0.2	0.1	224	18.0	14.2	2.7	7	5.3	3.5	46	2.4	11.5
EK-55	26	0.2	15.1	1.5	0.5	1.6	127.4	0.2	0.1	324	48.7	18.5	0.6	4	9	6.4	40	1.4	36.7
EK-56	9	1.1	12.3	0.3	0.2	10.6	82.7	0.2	0.1	272	7.5	9.7	12.0	12	26.1	9.8	49	2.7	41.8
Mafic dykes																			
EK-47	10	0.8	14.6	0.4	0.2	2.7	108.1	0.2	0.1	426	10.6	9.8	1.2	13	163.5	7.1	54	1.8	41.6
EK-48	15	1.9	14.1	0.8	0.3	2.3	94.2	0.2	0.1	339	25.2	14.0	0.7	7	58.3	37.9	46	1.4	49.3
Standard																			
STD SO-18	520	6.9	18	10	22	29.1	423.3	10.3	16.8	215	293.4	32.1	<0.1	<1	<0.1	<0.1	25	<0.1	28.5

bias correction was applied on the measured Sr and Nd isotope data. Quality control of the Sr and Nd isotope analyses was checked by applying the same procedures to the USGS rock standards. During the period of analyses, the AGV-1 USGS standard gave $^{87}Sr/^{86}Sr = 0.703993 \pm 12$ ($n = 2$) and $^{143}Nd/^{144}Nd = 0.512784 \pm 3$ ($n = 2$) and the G2 USGS standard gave $^{87}Sr/^{86}Sr = 0.709775 \pm 10$ ($n = 2$) and $^{143}Nd/^{144}Nd = 0.512224 \pm 3$ ($n = 2$), respectively.

Separation and column chromatography of Pb were performed in Teflon columns in a BioRad AG1-X8 anion exchange resin by using HBr–HCl ion exchange method. Lead was collected after successively adding HCl and HBr

Table 3 Rare-earth element compositions of the rock units in the study area

	La ppm	Ce ppm	Pr ppm	Nd ppm	Sm ppm	Eu ppm	Gd ppm	Tb ppm	Dy ppm	Ho ppm	Er ppm	Tm ppm	Yb ppm	Lu ppm	$(Eu/Eu^*)_N$	$(La/Yb)_N$	Nb/Yb
Plagiogranites																	
EK-34	3.0	8.5	1.55	8.4	3.06	0.70	4.36	0.91	5.76	1.34	4.25	0.69	4.58	0.74	0.58	0.44	0.20
EK-40	1.9	5.8	0.99	5.7	1.96	0.76	2.93	0.61	4.09	0.91	2.67	0.44	2.79	0.47	0.97	0.46	0.25
EK-41	1.7	5.5	1.00	5.8	2.17	0.69	3.28	0.67	4.46	1.00	3.08	0.49	3.20	0.51	0.79	0.36	0.22
EK-44	2.1	5.8	1.14	6.8	2.90	0.80	4.56	0.93	6.35	1.43	4.25	0.66	4.27	0.64	0.67	0.33	0.16
EK-49	2.0	6.3	1.16	7.0	2.62	0.75	4.15	0.83	5.65	1.28	3.86	0.63	3.97	0.63	0.69	0.34	0.18
Gabbros																	
EK-30	0.8	1.8	0.34	1.8	0.69	0.39	1.09	0.25	1.47	0.35	1.05	0.17	1.13	0.17	1.37	0.48	0.18
EK-33	1.2	3.3	0.63	3.5	1.36	0.39	2.47	0.58	4.02	0.95	2.92	0.46	3.04	0.51	0.65	0.27	0.20
EK-36	0.5	1.5	0.32	1.9	0.89	0.25	1.57	0.35	2.33	0.53	1.59	0.26	1.75	0.30	0.64	0.19	0.17
EK-55	2.6	6.4	1.17	5.8	1.98	0.76	2.58	0.51	3.25	0.73	2.12	0.33	2.03	0.32	1.02	0.87	0.25
EK-56	0.4	1.2	0.25	1.6	0.71	0.32	1.15	0.24	1.65	0.38	1.12	0.18	1.16	0.19	1.08	0.23	0.17
Mafic dykes																	
EK-47	0.5	1.4	0.26	1.6	0.68	0.31	1.19	0.23	1.71	0.38	1.12	0.19	1.18	0.19	1.05	0.29	0.17
EK-48	1.5	4.0	0.70	3.9	1.39	0.58	2.01	0.38	2.57	0.52	1.49	0.24	1.47	0.23	1.06	0.69	0.20
Standard																	
STD SO-18	12.4	27	3.45	14	2.99	0.9	2.98	0.52	3.00	0.62	1.84	0.29	1.8	0.28			

Table 4 Normative mineralogy of the plagiogranite samples from the study area

	EK-34	EK-40	EK-41	EK-44	EK-49
Quartz	46.50	40.83	40.43	37.74	42.81
Anorthite	11.92	19.93	21.36	19.93	19.18
Diopside	0.00	0.00	0.00	0.45	0.00
Sphene	0.00	0.00	0.06	0.64	0.00
Hypersthene	0.72	1.28	1.75	2.23	1.99
Albite	37.33	33.95	30.77	33.45	30.41
Orthoclase	1.14	1.59	3.11	2.56	2.64
Apatite	0.06	0.14	0.14	0.14	0.12
Ilmenite	0.14	0.10	0.11	0.13	0.11
Corundum	0.88	0.31	0.00	0.00	0.41
Rutile	0.02	0.14	0.14	0.00	0.15
Hematite	1.31	1.72	2.12	2.73	2.18

following a procedure modified after Romer et al. (2001). Lead was loaded with silica gel and 0.005 N H_3PO_4 on single filaments and measured at 1250–1350 °C in a static mode. NIST SRM981 measured during the analyses, which gave 16.916, 15.470 and 36.645 ($n = 4$) for $^{206}Pb/^{204}Pb$, $^{207}Pb/^{204}Pb$ and $^{208}Pb/^{204}Pb$, respectively, and necessary corrections were made on the results. AGV-2 and BCR-2 USGS reference materials were also processed and measured in the same period, and results are given in Table 6. The Pb isotope data obtained from the USGS reference materials are comparable with the data in the literature (e.g., mean data of Weiss et al. 2006; Table 6). All isotopic ratios were measured by using a Thermo-Fisher Triton thermal ionization mass spectrometer, and standard errors were presented in 2-sigma level.

Geochemistry

The geochemical data, including Sr, Nd and Pb isotopes, are presented in Tables 1, 2, 3, 4, 5, 6. Previously published geochemical data from plagiogranites in the study area (i.e., Göncüoglu and Türeli 1993a) including major elements with limited trace elements (Rb, Sr, Ba, Zr, Y and Nb) and data from two plagiogranite samples from the study area (EK-40 and 41) (i.e., Grimes et al. 2013) are broadly similar to the results presented in this study; thus, these data were not taken into account to get rid of repetition.

Hydrothermal alteration and even very low-grade metamorphism that could modify chemical composition are probable for most of the ophiolitic rocks. Therefore, before geochemical interpretations the behavior of specific elements during alteration is taken into account. As the SiO_2 and Al_2O_3 contents of the rocks are plotted against silicification index (SI), pronounced linear trends indicating absence of silicification and/or loss of SiO_2 among the samples within each group are obtained (Fig. 5a, b). Moreover, there is no correlation of SiO_2 content to $100*(K_2O+MgO)/(K_2O+MgO+Na_2O+CaO)$ (AI) and Al_2O_3/Na_2O (SDI) within each rock group that promotes no modification in SiO_2 of the rocks (Fig. 5c, d). The rocks least altered are negligible in MgO/FeO ratio (Coish et al. 1983), but plot of $Al_2O_3/$

Table 5 Strontium and neodymium isotopic compositions of the rock units in the study area

	$^{87}Sr/^{86}Sr_{(m)}$	Rb (ppm)	Sr (ppm)	$^{87}Sr/^{86}Sr^{a}_{(T)}$	$^{143}Nd/^{144}Nd_{(m)}$	Nd (ppm)	Sm (ppm)	$^{143}Nd/^{144}Nd^{a}_{(T)}$	$\varepsilon Nd^{a}_{(T)}$
Plagiogranites									
EK-34	0.705971 ± 10	2.3	102.3	0.705888	0.512958 ± 14	8.4	3.06	0.512828	6.0
EK-40	0.704840 ± 9	9.1	103.4	0.704514	0.512966 ± 6	5.7	1.96	0.512844	6.3
EK-41	0.704675 ± 7	10.5	80.6	0.704193	0.513042 ± 16	5.8	2.17	0.512909	7.5
EK-44	0.704521 ± 8	7.0	77.5	0.704187	0.513018 ± 11	6.8	2.90	0.512866	6.7
EK-49	0.705076 ± 5	13.8	84.1	0.704469	0.512996 ± 7	7.0	2.62	0.512863	6.6
Gabbros									
EK-33	0.705635 ± 28	2.0	241.1	0.705605	0.513008 ± 4	3.5	1.36	0.512870	6.8
EK-36	0.705990 ± 24	1.8	151.1	0.705946	0.513005 ± 12	1.9	0.89	0.512838	6.2
Mafic dykes									
EK-47	0.706565 ± 32	2.7	108.1	0.706473	0.513019 ± 11	1.6	0.68	0.512868	6.7
EK-48	0.704694 ± 11	2.3	94.2	0.704604	0.513003 ± 3	3.9	1.39	0.512876	6.9

Elemental compositions are from Tables 2 and 3

[a] $T = 90$ Ma

Na_2O against MgO/FeO for the studied rocks displays that two gabbro samples with higher MgO/FeO ratio scatter from the linear trend (Fig. 5e). This might be due to low magmatic FeO content of the samples (EK-33 and EK-36) rather than alteration because these two samples lie in the least altered rock field of Large et al. (2001) on the 100*(MgO+FeO)/(MgO+FeO+Na_2O+K_2O) (CCPI) against AI diagram (Fig. 5f) and in fresh to weakly altered field of Spitz and Darling (1978) on Al_2O_3/Na_2O vs. Na_2O diagram (Fig. 5g). Lower AI values of plagiogranites and higher CCPI values of few mafic samples compared to least altered rocks of Large et al. (2001) on the CCPI against AI diagram might be related to primary mineral content rather than sericite chlorite alteration (Fig. 5f). Alkali mobility that might result from spilitization and K-metasomatism is also evaluated by plotting on $K_2O + Na_2O$ vs. $K_2O/(K_2O + Na_2O)$ diagram of Hughes (1973). The samples almost lie in or near igneous spectrum field that infer no alteration (Fig. 5h). This assumption is well supported by plot of plagiogranites in fresh to weakly altered field of Spitz and Darling (1978) in Al_2O_3/Na_2O vs. Na_2O diagram (Fig. 5g). Both in $K_2O + Na_2O$ vs. $K_2O/(K_2O + Na_2O)$ and Al_2O_3/Na_2O vs. Na_2O diagrams, the rock types show pronounced linear trends within each group supporting lack of significant alteration. Chemical index of alteration ($Al_2O_3/(Al_2O_3 + Na_2O + K_2O + CaO)$ of the rocks (plagiogranite: 62–65, mafic rock: 47–59) also supports that chemical alteration is not significant (fresh mafic rocks: 30–45 and fresh felsic rocks: 45–55, Fedo et al. 1995). However, the sample EK-48 showing scatter in SiO_2, Al_2O_3, MgO/FeO from mafic trends might be slightly affected by alteration. Additionally plagiogranite sample EK-34 also differs from other plagiogranite samples, which may be related to its higher albite content (i.e., chemical composition) or slight albitization alteration effect.

Although alteration is inconsequential, the behavior of some critical elements against Zr/TiO_2 is also controlled (Fig. 6) regarding the immobile nature of high field strength elements (HFSE) (e.g., Zr, Nb, Ti, Hf, Y) (e.g., Pearce 1983). Variation of several elements against Zr/TiO_2 as a discrimination factor shows that alteration is not significant (Fig. 6). Only two samples (EK-34: plagiogranite and EK-48: mafic dyke) display slight effect of alteration for Rb and Sr.

On the $Na_2O + K_2O$ versus SiO_2 classification of Irvine and Baragar (1971) all samples plot in the subalkaline field (not shown). On the ternary diagram (FeO*–Na_2O–K_2O) of Irvine and Baragar (1971), plagiogranite samples show calc-alkaline trend, while mafic dyke and gabbro samples have tholeiitic affinity (not shown).

The samples from plagiogranites in the Ekecikdağ area are characterized by their high SiO_2 (69.87–75.92 wt%) and remarkably low K_2O (less than 0.5 wt%) contents (Table 1; Fig. 7), which are typical for oceanic plagiogranites (Coleman and Peterman 1975). They have extremely low orthoclase content and plot in the tonalite and trondhjemite fields on the normative Ab–An–Or diagram (Table 4; Fig. 8a). Their moderate to high Na_2O (3.4–4.2 wt%) and CaO (2.4–4.5 wt%) contents, moderate to low Al_2O_3 contents (12.8–14.3 wt%), besides low TiO_2 (less than 0.45 wt%) and MgO (less than 1.14 wt%) contents are also consistent with the common definition of oceanic plagiogranites (e.g., Coleman and Peterman 1975; Arth 1979; Coleman and Donato 1979).

Concerning major elements, gabbros and mafic dykes significantly differ from plagiogranites with their lower SiO_2 and Na_2O, besides higher Al_2O_3, MgO and CaO contents (Table 1; Fig. 7). Major element characteristics of gabbros and mafic dykes are broadly similar to each

Table 6 Lead isotopic compositions of the rock units in the study area together with those of the AGV-2 and BCR-2 USGS standards

	$^{206}Pb/^{204}Pb_{(m)}$	$^{207}Pb/^{204}Pb_{(m)}$	$^{208}Pb/^{204}Pb_{(m)}$	Th[b] (ppm)	U (ppm)	Pb (ppm)	$^{206}Pb/^{204}Pb^{a}_{(T)}$	$^{207}Pb/^{204}Pb^{a}_{(T)}$	$^{208}Pb/^{204}Pb^{a}_{(T)}$
Plagiogranites									
EK-40	18.4966	15.5943	38.4350	0.2	0.2	0.6	18.1987	15.5801	38.3373
Standard error[c]	0.0011	0.0010	0.0026						
EK-41	18.4820	15.5783	38.3898	0.2	0.1	0.6	18.3332	15.5712	38.2922
Standard error	0.0072	0.0061	0.0149						
EK-44	18.4916	15.5847	38.4322	0.2	0.1	0.9	18.3924	15.5800	38.3671
Standard error	0.0017	0.0014	0.0034						
EK-49	18.5880	15.6228	38.5846	0.3	0.2	1.0	18.4086	15.6142	38.4964
Standard error	0.0024	0.0021	0.0051						
Gabbros									
EK-33	18.6561	15.6429	38.6540	0.2	0.1	1.2	18.5812	15.6393	38.6049
Standard error	0.0092	0.0077	0.0190						
EK-36	18.5739	15.6340	38.6024	0.2	0.1	2.7	18.5407	15.6324	38.5806
Standard error	0.0008	0.0007	0.0017						
Mafic dykes									
EK-47	18.5651	15.6051	38.5043	0.2	0.1	1.2	18.4905	15.6016	38.4553
Standard error	0.0011	0.0009	0.0022						
EK-48	18.5859	15.6445	38.6141	0.2	0.1	0.7	18.4576	15.6383	38.5300
Standard error	0.0025	0.0020	0.0051						
USGS standards measured during the period of analyses									
AGV-2 ($n = 3$)	18.8655	15.6124	38.5228						
Standard error	0.0174	0.0205	0.0697						
BCR-2 ($n = 4$)	18.7512	15.6277	38.7239						
Standard error	0.0141	0.0163	0.0573						
USGS standards reported by Weiss et al. (2006)									
AGV-2	18.8688	15.6173	38.5443						
Standard error	0.0063	0.0071	0.0135						
BCR-2	18.7529	15.6249	38.7237						
Standard error	0.0195	0.0040	0.0405						

[a] $T = 90$ Ma

[b] Elemental compositions are from Table 2

[c] Standard errors are in 2-sigma level

other (Table 1; Fig. 7). On the Zr/TiO_2 vs. Nb/Y diagram all samples show subalkaline character (Fig. 8b). Mafic dyke samples plot in subalkaline basalt field, while gabbro samples plot in subalkaline basalt to andesite/basalt field (Fig. 8b) that infer diorite-gabbro transitional composition.

All samples show LILE enrichment with respect to N-MORB (normalization after Sun and McDonough 1989), but Rb, Ba, K are fairly enriched in plagiogranites (Fig. 9a). Nb and Ti depletion with respect to N-MORB is common for all samples, while Nb content is higher in plagiogranites (Fig. 9a). Additionally, V and Sc are lower; Hf, Y, Zn and Zr are generally higher in plagiogranites (Table 2; Fig. 7) with respect to gabbros and mafic dykes. Ekecikdağ ophiolitic rocks broadly coincide with the trends of both back-arc and fore-arc SSZ ophiolites (after Metcalf and Shervais 2008). The rocks show broadly similar concave upward to flat patterns in N-MORB-normalized REE diagram (Fig. 9b). Gabbros and mafic dyke samples almost show depletion in all REE with mild depletion in LREE with respect to N-MORB (Fig. 9b), while plagiogranites are generally enriched both in LREE and in HREE with respect to other samples. Plagiogranites show negative Eu anomalies ($[Eu/Eu^*]_N = 0.58–0.97$), which infer retention of Eu by remaining plagioclase in source rock (Table 3). Conversely, mafic dykes lack Eu anomaly (1.05–1.06) that point out a plagioclase-poor residue. Gabbro samples, on the other hand, show a large range of Eu anomalies from negative to positive (0.64–1.37). The negative Eu anomaly in the gabbros may point to plagioclase fractionation

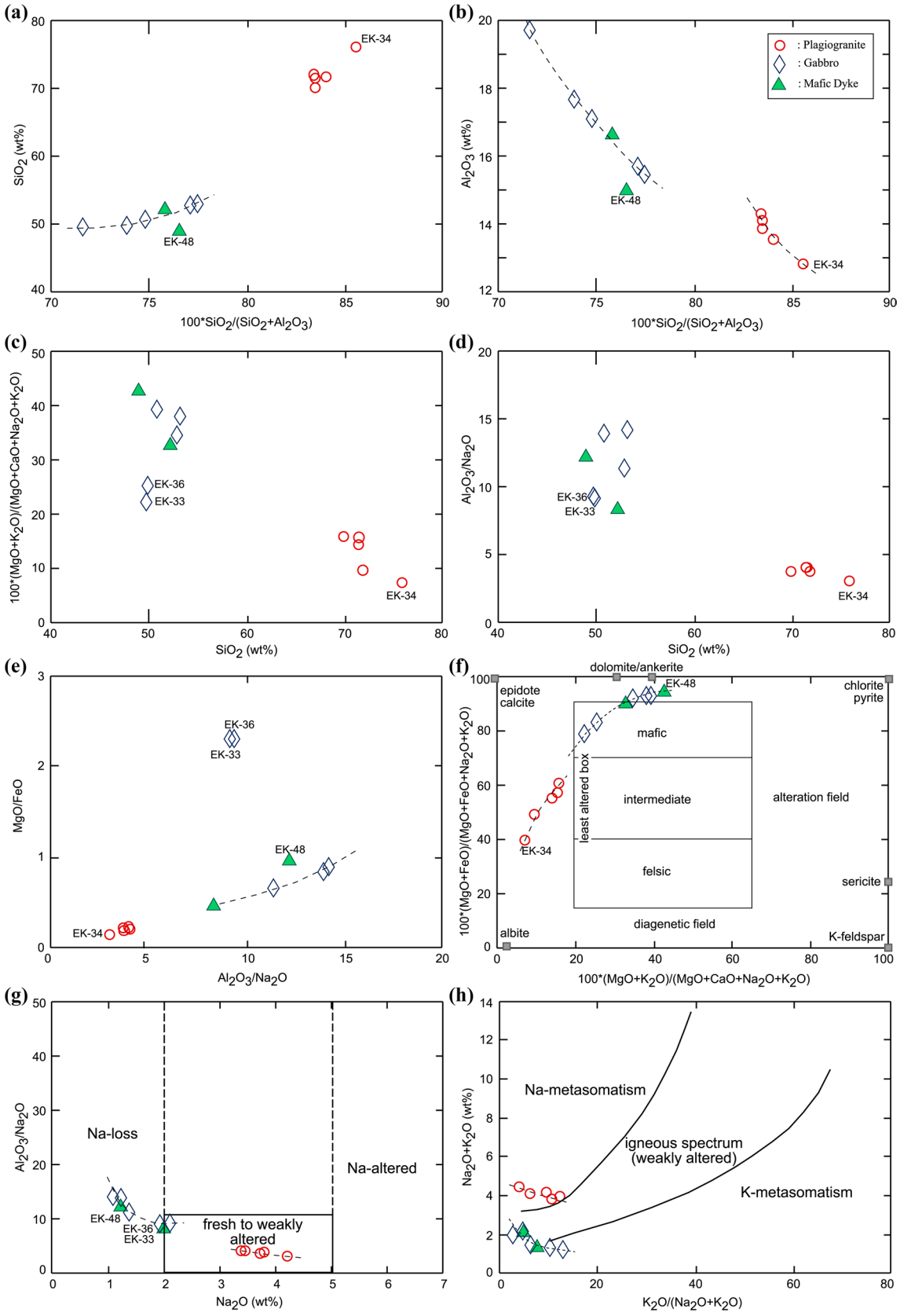
(a)
SiO2 (wt%)
100*SiO2/(SiO2+Al2O3)
EK-34
EK-48
(b)
Al2O3 (wt%)
100*SiO2/(SiO2+Al2O3)
: Plagiogranite
: Gabbro
: Mafic Dyke
EK-48
EK-34
(c)
100*(MgO+K2O)/(MgO+CaO+Na2O+K2O)
SiO2 (wt%)
EK-36
EK-33
EK-34
(d)
Al2O3/Na2O
SiO2 (wt%)
EK-36
EK-33
EK-34
(e)
MgO/FeO
Al2O3/Na2O
EK-36
EK-33
EK-48
EK-34
(f)
100*(MgO+FeO)/(MgO+FeO+Na2O+K2O)
100*(MgO+K2O)/(MgO+CaO+Na2O+K2O)
dolomite/ankerite
epidote
calcite
chlorite
pyrite
mafic
intermediate
felsic
least altered box
alteration field
sericite
albite
diagenetic field
K-feldspar
EK-48
EK-34
(g)
Al2O3/Na2O
Na2O (wt%)
Na-loss
Na-altered
fresh to weakly
altered
EK-48
EK-36
EK-33
(h)
Na2O+K2O (wt%)
K2O/(Na2O+K2O)
Na-metasomatism
igneous spectrum
(weakly altered)
K-metasomatism

◂**Fig. 5** Alteration index diagrams **a** SiO_2 versus 100* $SiO_2/(SiO_2 + Al_2O_3)$, **b** Al_2O_3 versus 100* $SiO_2/(SiO_2 + Al_2O_3)$, **c** 100*(MgO + K_2O)/(MgO + CaO + Na_2O + K_2O) versus SiO_2, **d** Al_2O_3/Na_2O versus SiO_2, **e** MgO/FeO versus Al_2O_3/Na_2O, **f** 100*(MgO + FeO)/(MgO + FeO + Na_2O + K_2O) versus 100*(MgO + K_2O)/(MgO + CaO + Na_2O + K_2O) (least altered *box* by Large et al. (2001)), **g** Al_2O_3/Na_2O versus Na_2O (fresh to weakly altered *box* by Ruks et al. (2006)), **h** Na_2O + K_2O versus $K_2O/(Na_2O + K_2O)$ (igneous spectrum field by Hughes (1973))

during gabbro crystallization; on the other hand, accompanying positive Eu anomaly is likely to be result of the existence of plagioclase in the gabbros. $(La/Yb)_N$ varies with 0.33 to 0.46 in plagiogranites, from 0.19 to 0.87 in gabbros and 0.29 to 0.69 in mafic dykes (Table 3). Consequently geochemistry of the studied ophiolitic rocks suggests depleted source which was modified by a subduction component (e.g., Nb- and Ti-negative anomalies). Furthermore, Sarıkaraman plagiogranites at the east of the study area reveal similar multielement variation trends with the Ekecikdağ plagiogranite (Fig. 10). Geochemical similarities between Sarıkaraman and Ekecikdağ plagiogranites are also detected in Fig. 7, where Ekecikdağ plagiogranite samples plot next to Sarıkaraman plagiogranite data from Floyd et al. (1998).

On the Nb vs Y diagram (Pearce et al. 1984a) plagiogranites from the study area plot close to the fields of Evros, Oman, Troodos and Sarıkaraman ophiolitic rocks (Fig. 11). The plagiogranites reveal similar petrographic and geochemical characteristics to other well-studied plagiogranites from different ophiolitic rocks in the world. However, the abundance of Nb (less than 1 ppm) is distinctly lower than the other ophiolitic bodies (Fig. 11). The common characteristics of these suites are their SSZ origin (e.g., Pearce et al. 1984b; Bonev and Stampfli 2009).

On the Nb/La versus La/Yb diagram from Hollocher (2012) plagiogranites, together with gabbros and mafic dyke samples, are distributed from highly depleted MORB to oceanic arc fields with sediment-poor ocean subduction component (Fig. 12a). Nb/Yb ratios of all samples range from 0.10 to 0.25 (Table 2), which point out N-MORB source rather than E-MORB (e.g., Pearce 2008). Moreover, TiO_2/Yb values range between 0.03 and 0.50 and are below the OIB array (deep melting) of Pearce (2008). Th/Yb versus Nb/Yb (Fig. 12b) diagram of Pearce (2008) reveals this depletion, but in this diagram increase in Th/Yb ratio due to subduction component is noteworthy.

On the SiO_2–TiO_2–K_2O ternary diagram (Fig. 12c) plagiogranites plot in the field of gabbro anatexis; on the other hand, gabbros and mafic dyke samples show distribution near to ophiolitic rocks from Oman (Grimes et al. 2013). Furthermore, on the TiO_2 versus SiO_2 diagram (Koepke et al. 2007), all samples plot in partial melting field of mid-ocean ridge gabbros producing silicic magmas (Fig. 12d). Therefore, partial melting of gabbro is suggested as a probable process for the generation of the Ekecikdağ plagiogranite (e.g., Fig. 12c, d).

In multielement variation diagrams (Fig. 9a), samples from the Ekecikdağ ophiolitic rocks generally show high LILE/HFSE ratios, especially for plagiogranites, where LILE contents are generally higher than N-MORB, and HFSE contents are somewhat less than and/or almost identical to those of N-MORB. This trend is an indication for their difference from N-MORB source and is the case observed in both fore-arc and back-arc SSZ environments (e.g., Metcalf and Shervais 2008) (Fig. 9). Significant enrichment of molybdenum in plagiogranites (e.g., 2.2–6.1 ppm, Table 2), on the other hand, can be related to differentiation from mafic magma or secondary hydrothermal effects (e.g., Kuroda and Sandell 1954). Diagrams related to alteration revealed that the hydrothermal effects are not significant in the Ekecikdağ ophiolitic rocks; therefore, differentiation from mafic magma is likely to be the case recorded from molybdenum contents. However, effects of hydrous components which could further modify the geochemical nature cannot be disregarded as seen on Th/Yb versus Nb/Yb diagram (Fig. 12b).

Depletion of trace elements detected in the Ekecikdağ ophiolitic rocks is consistent with their SSZ origin (e.g., Pearce et al. 1984a). Furthermore, deviation of the chemical features of the Ekecikdağ ophiolitic rocks from N-MORB chemistry (e.g., Figs. 9, 12) implies that secondary effects were raised due to contamination by hydrothermally altered crust at the base of the sheeted dike complex and in the upper gabbros (e.g., Grimes et al. 2013) and/or metasomatic agents derived from a subducted slab during supra-subduction event (e.g., Toksoy-Köksal et al. 2009a).

Isotope geochemistry

Measured and initial whole-rock isotope data are presented in Tables 5 and 6. For the initial $^{87}Sr/^{86}Sr$ ratio calculation 90 Ma is used. This is the age of the Sarıkaraman plagiogranite (e.g., Yalınız et al. 1999; van Hinsbergen et al. 2016), which is accepted to be the equivalent of the Ekecikdağ plagiogranite regarding the identical geological setting (e.g., Fig. 1) and geochemical character (Figs. 7, 10, 11).

The initial $^{87}Sr/^{86}Sr$ ratios of plagiogranites in the study area range from 0.704187 to 0.705888 (Table 5). The range of this ratio is 0.705605–0.705946 for gabbros and 0.704604–0.706473 for mafic dykes (Table 5). Additionally, the initial $^{143}Nd/^{144}Nd$ ratios range between 0.512828 and 0.512909 for plagiogranites, 0.512838 and

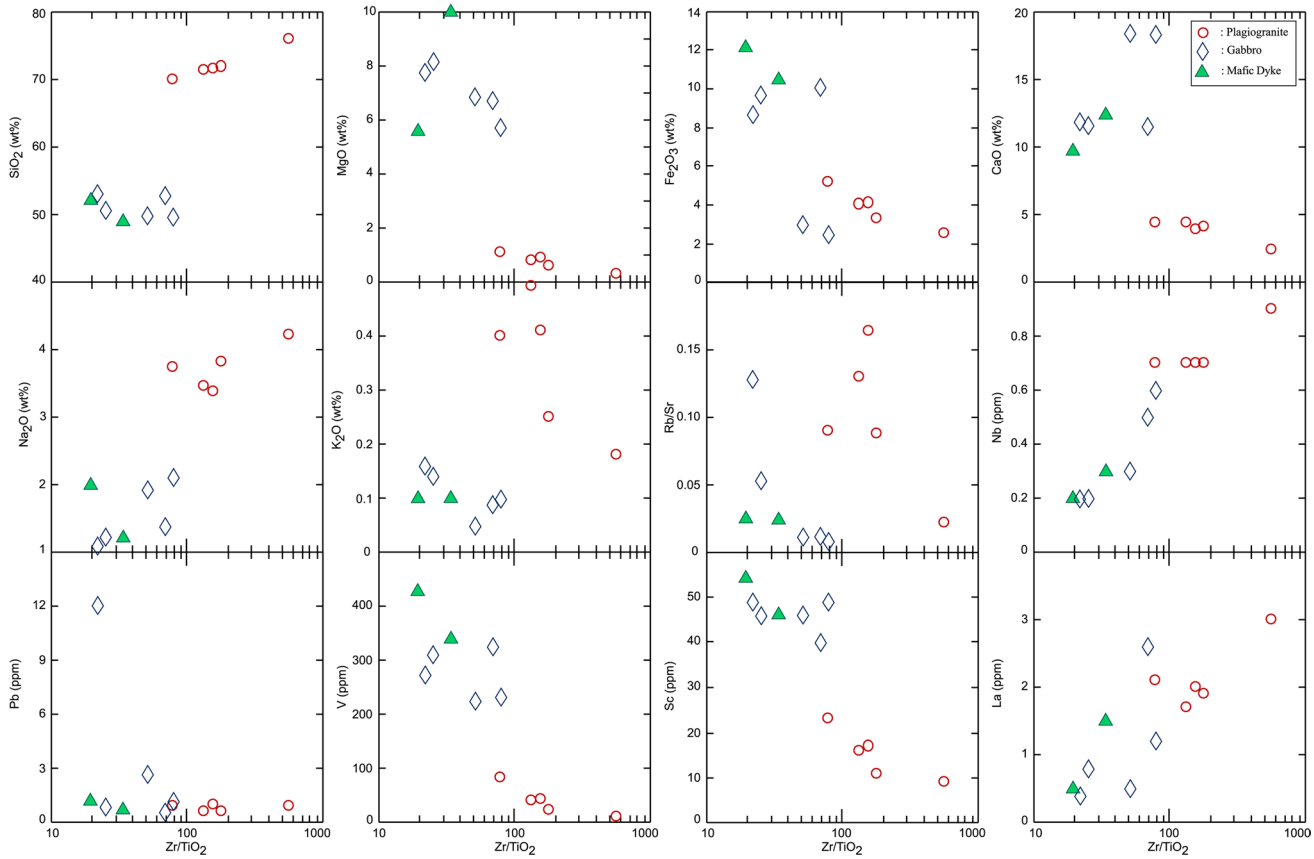

Fig. 6 Elemental variation diagrams for investigating alteration in the Ekecikdağ ophiolitic rocks. Selected elements plot against Zr/TiO_2

0.512870 for gabbros and 0.512868 and 0.512876 for mafic dykes. Neodymium isotope data of the Ekecikdağ ophiolitic rocks are of a very limited range and comparable to those of N-MORB (e.g., 0.512992–0.513269, Chauvel and Blichert-Toft 2001; 0.513083 ± 0.000020, Gale et al. 2013). However, Sr isotope data show some scatter especially for mafic dyke samples and one plagiogranite sample reaching considerably higher ratios than those of N-MORB (e.g., 0.702540–0.702920, Dupré and Allègre 1980; 0.702807 ± 0.000078, Gale et al. 2013). To sum up high initial Nd and generally low initial Sr isotopic compositions of the Ekecikdağ ophiolitic rocks point out their mantle origin.

The initial lead isotopic data of plagiogranites display non-scattered $^{206}Pb/^{204}Pb$ (18.199–18.409), $^{207}Pb/^{204}Pb$ (15.571–15.614) and $^{208}Pb/^{204}Pb$ (38.292–38.496) ratios (Table 6). Gabbros reveal (18.541–18.581), (15.632–15.639) and (38.581–38.605) ranges for $^{206}Pb/^{204}Pb$, $^{207}Pb/^{204}Pb$ and $^{208}Pb/^{204}Pb$ ratios, respectively (Table 6). Moreover, mafic dyke samples have (18.458–18.490), (15.602–15.638) and (38.455–38.530) ranges for $^{206}Pb/^{204}Pb$, $^{207}Pb/^{204}Pb$ and $^{208}Pb/^{204}Pb$ ratios, respectively (Table 6). As a conclusion, all of the rock types in the area are isotopically similar to each other and show slightly higher Pb/Pb isotope data with respect to the mean N-MORB Pb isotope data presented by Gale et al. (2013) (i.e., 18.298 ± 0.082, 15.505 ± 0.009, 37.992 ± 0.086, for $^{206}Pb/^{204}Pb$, $^{207}Pb/^{204}Pb$ and $^{208}Pb/^{204}Pb$ ratios, respectively).

On the $\varepsilon Nd_{(T)}$ vs. $^{87}Sr/^{86}Sr_{(T)}$ diagram (Fig. 13) the Ekecikdağ plagiogranites together with gabbros and mafic dykes reveal depleted source character, showing no tendency to enriched mantle reservoirs. They distribute close to the Nd–Sr isotope data of the ophiolitic rocks from the surrounding areas within the Eastern Mediterranean region such as the Eastern Vardar Zone, Samothraki and Troodos. Although limited, Nd–Sr isotope data from the Late Cretaceous (95 Ma) Stepanavan calc-alkaline lavas, which were suggested to be formed in a SSZ environment in the Lesser Caucaus (Armenia) (e.g., Rolland et al. 2009), also plot in nearby areas. Additionally, Nd–Sr isotopes of Iran ophiolites from Gogher-Baft and Neyriz (Shafaii Moghadam et al. 2013) together with the altered Oman lavas (Godard et al. 2006) plot in adjacent areas with the Ekecikdağ

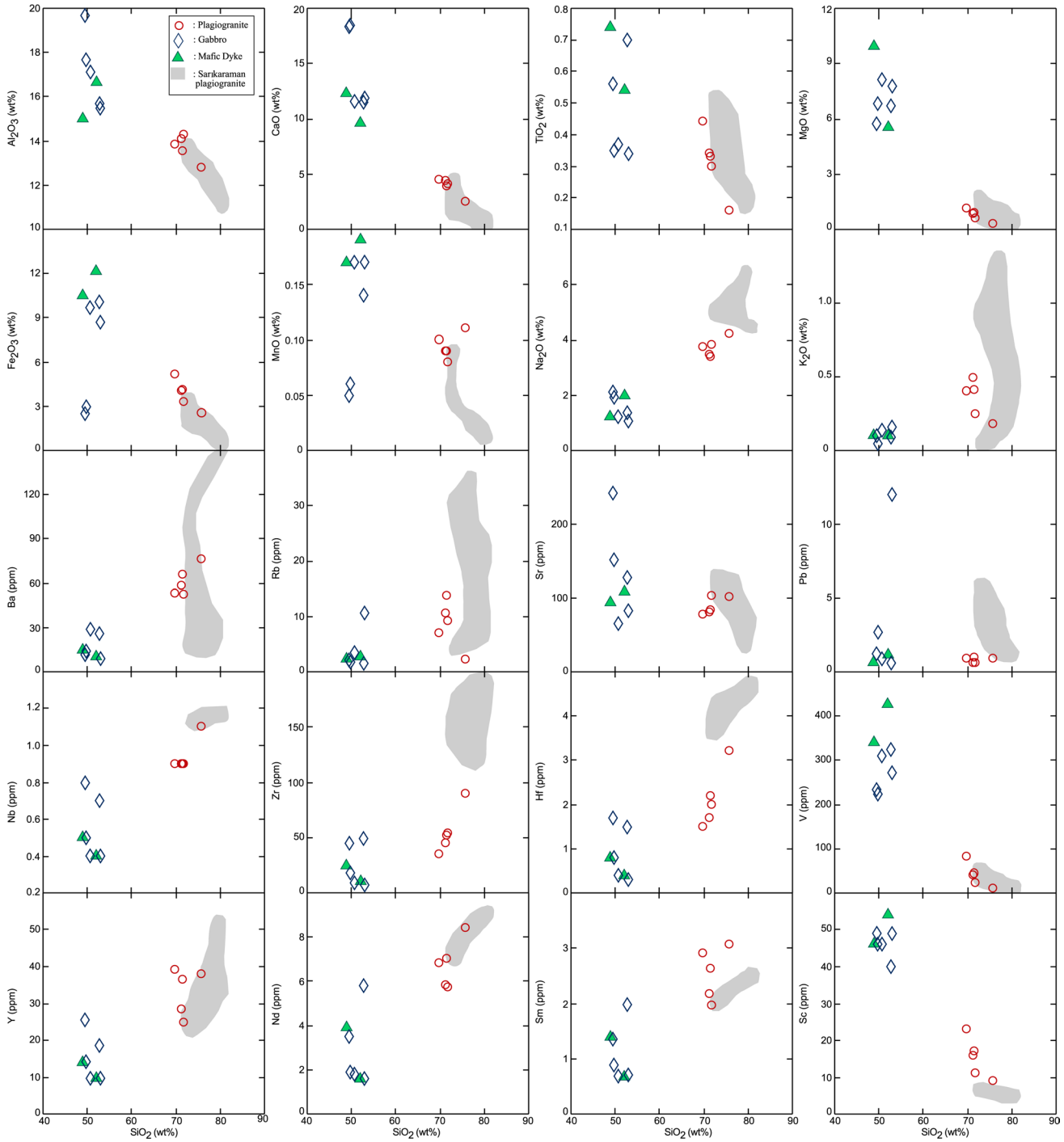

Fig. 7 Variation diagrams of selected elements against SiO_2. Sarıkaraman plagiogranites data are from Floyd et al. (1998)

ophiolitic rocks and other ophiolitic rocks from the Eastern Mediterranean (Fig. 13). The $\varepsilon Nd_{(T)}$ data from Dehshir ophiolite in Iran range from 6.44 to 8.31 (Shafaii Moghadam et al. 2012), which also coincide with the isotopic composition of the Ekecikdağ ophiolitic rocks. The notable scatter in $^{87}Sr/^{86}Sr$ isotope data of one plagiogranite (EK-34) and one mafic dyke (EK-48) sample could be related to the limited mobility of Rb and Sr under low-temperature seafloor alteration and is also observed in other ophiolitic suites (e.g., Hoernle 1998). Nevertheless, four plagiogranite samples cluster in a narrow initial Sr isotope data range from 0.70418 to 0.70451. Least altered mafic

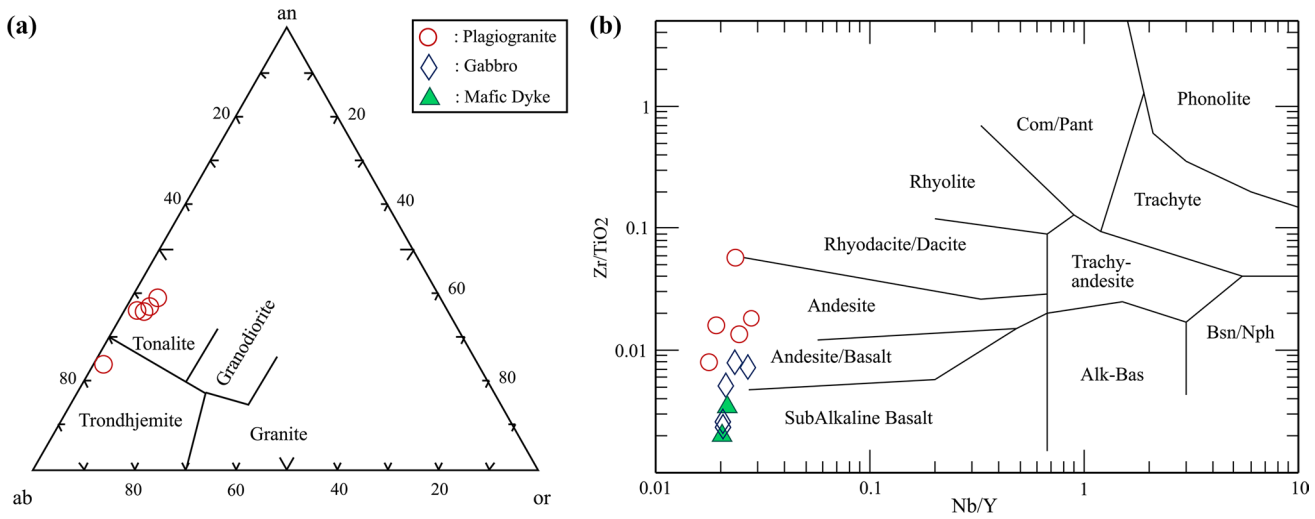

Fig. 8 **a** Normative albite (ab)-anorthite (an)-orthoclase (or) ternary diagram (Barker 1979) of Ekecikdağ plagiogranites, **b** Zr/TiO_2 versus Nb/Y diagram (Winchester and Floyd 1977) of the Ekecikdağ ophiolitic rocks

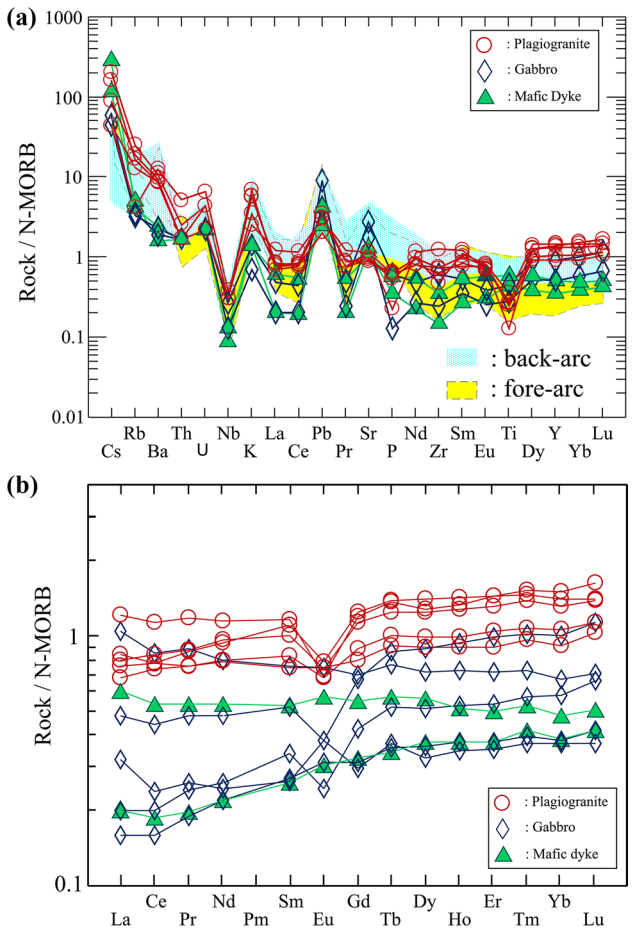

Fig. 9 **a** N-MORB normalized (after Sun and McDonough 1989) multielement diagrams for the Ekecikdağ ophiolitic rocks, fore-arc and back-arc SSZ ophiolitic rocks areas are from Metcalf and Shervais (2008), **b** N-MORB normalized (after Sun and McDonough 1989) rare-earth element patterns for the Ekecikdağ ophiolitic rocks

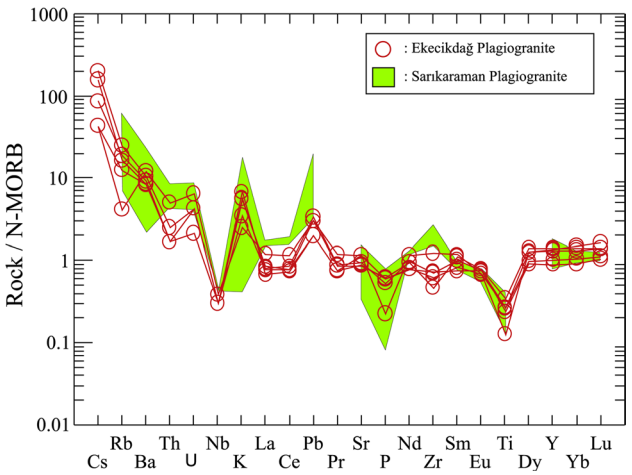

Fig. 10 N-MORB-normalized (after Sun and McDonough 1989) multielement diagrams for the Ekecikdağ and Sarıkaraman plagiogranites

dyke sample (EK-47) reveals highest initial $^{87}Sr/^{86}Sr$ ratio among the studied samples, but it is difficult to constrain the Sr isotopic nature of all mafic dykes in the area owing to the limited isotope data. Nd isotope data from both of the mafic dyke samples are not only close to each other but also akin to other ophiolitic rock samples concerned in this study. Hence, it is plausible to propose similar isotopic source characteristics for both of the mafic dyke samples.

The lead isotope data plot above the NHRL and show compositions akin to the other Eastern Mediterranean ophiolitic rocks, i.e., Troodos, Baer Bassit and Oman ophiolitic rocks (Fig. 14). It is notable in these diagrams that the Pb isotope data from Gogher-Baft ophiolites (Iran), which was

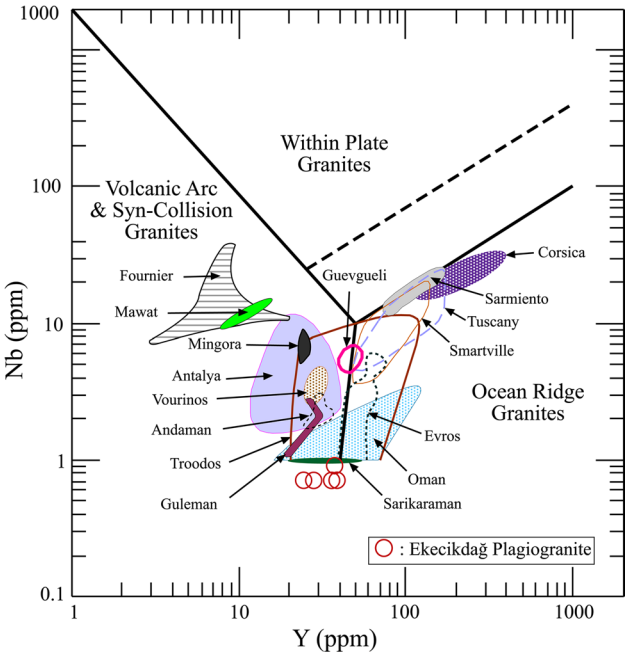

Fig. 11 Nb versus Y diagram (Pearce et al. 1984a) of the Ekecikdağ plagiogranites. Fields of other plagiogranites: Mingora (*3*) (Barbieri et al. 1994), Oman (*5*), Troodos (*27*), Antalya (*8*), Smartville (*7*), Vourinos (*4*), Tuscany (*9*), Sarmiento (*8*), Corsica (*10*) (Pearce et al. 1984a and references therein); Evros (*6*) (Magganas 2007); Guevgueli (*3*) (Hatzipanagiotou and Tsikouras 1999), Mawat (*7*) (Mirza and Ismail 2007), Guleman (*3*) (Kılıç 2009), Andaman (*8*) (Jafri et al. 1995), Sarıkaraman (*9*) (Floyd et al. 1998), Fournier (*9*) (Brophy and Pu 2012). Italic numbers in parentheses indicate number of analyzed plagiogranite samples

described as fore-arc ophiolitic rocks (e.g., Shafaii Moghadam et al. 2013), almost coincide with the data from the study area. The Ekecikdağ ophiolitic rocks do not plot in the field of enriched mantle sources, but they reveal relatively higher $^{207}Pb/^{204}Pb$ and $^{208}Pb/^{204}Pb$ ratios than average N-MORB and BAB isotope data (e.g., Gale et al. 2013). This modification may be related to the isotopic character carried by sediments accompanying the subducted oceanic crust during the previous subduction event (e.g., Workman et al. 2004). On the $^{143}Nd/^{144}Nd$ versus $^{206}Pb/^{204}Pb$ (Fig. 15) diagram, an isotopic source character that is not enriched as much as enriched mantle reservoirs but not depleted as N-MORB and BAB sources is remarkable.

When the Nd–Sr–Pb isotope data are evaluated together (Fig. 15), the Ekecikdağ ophiolitic rocks do not exactly plot in one of the source centers like DMM or EM. Therefore, it can be deduced that the ophiolitic Ekecikdağ rocks have an isotopic nature, which is a mixture of different components like DMM, HIMU (?) and EM as in the case of Hawaii ocean islands (e.g., Zindler and Hart 1986). However, effects of enrichment component(s) which may be sourced from trace element enriched pelagic or terrigenous sediments (e.g., Workman et al. 2004) might have been limited (e.g., Fig. 12a). Hence, they do not plot in the proximity of isotope data of EM-I or EM-II sources. This circumstance also supports the depleted origin of the Ekecikdağ ophiolitic rocks, which was modified by subduction fluids. Considering the $^{143}Nd/^{144}Nd$ versus $^{206}Pb/^{204}Pb$ data (Fig. 15) the SSZ-type Gogher-Baft ophiolitic rocks from Iran show relatively wide distribution, but mostly overlap with the Ekecikdağ isotope data.

Discussion

Disregarding the authors supporting a non-ophiolitic origin of the ultramafic and mafic rocks in Central Anatolia (e.g., İlbeyli 1993; Erdoğan et al. 1996; Kadıoğlu et al. 1998), there is now consensus that these rocks together with oceanic lavas and sediments are allochthonous members of a dismembered ophiolitic body. They have been named as the Central Anatolian Ophiolites (Göncüoglu et al. 1991; Göncüoglu and Türeli 1993a) and were subject of several studies (e.g., Floyd et al. 1998, 2000; Yalınız et al. 1999; Koçak et al. 2005, 2014). A number of studies were devoted to the origin of these rocks. For instance, Toksoy-Köksal et al. (2001) interpreted the Kurançalı phlogopitic metagabbro (Kırşehir, Central Anatolia) of the İAEO belt, in NW of the study area, to be generated from transitional back-arc basin/island arc basalt to island arc basalt-type oceanic crust affected by an alkaline metasomatism. Accordingly, Toksoy-Köksal et al. (2009a) suggested for the Kurançalı ultramafic–mafic cumulates crystallization from a metasomatized mantle source with high-K calc-alkaline character with alkaline affinity in an island arc basement in SSZ setting. Likewise, Yalınız et al. (1999) ascribed the ophiolitic rocks in Central Anatolia as fore-arc type based on their studies in the Sarıkaraman area at the east of the study area. In addition, Yalınız et al. (1996, 2000) defined the ophiolitic basalts in the Sarıkaraman area as island arc tholeiites formed in a SSZ setting, while the late dykes generated from N-MORB-type sources. For the Çiçekdağ Ophiolite in the northern part of the CACC, Yalınız et al. (2000) put forward a partial melting of already depleted oceanic lithosphere in a SSZ setting. Floyd et al. (2000) indicated that the SSZ-type ophiolitic rocks in Central Anatolia were formed as parts of an incipient arc with a limited contribution of back-arc spreading. Furthermore, Koçak et al. (2014) attributed the plagiogranite in the Bozkır area as the low-pressure partial melting products of hydrated oceanic gabbro. Recently, van Hinsbergen et al. (2016) support the idea that the Central Anatolian Ophiolites were derived from E to W and N to S striking segments

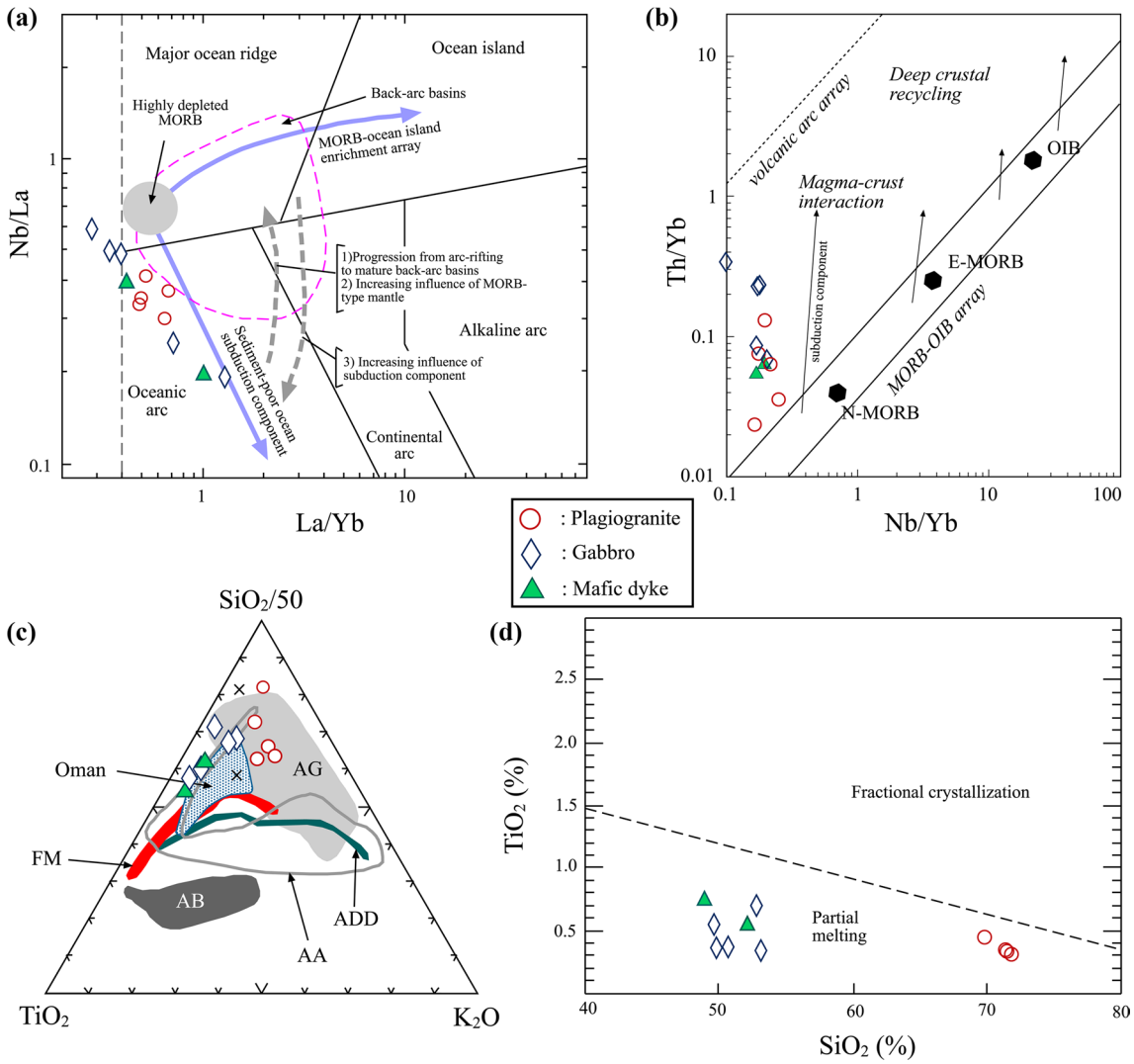

Fig. 12 **a** Nb/La versus La/Yb (Hollocher et al. 2012), **b** Th/Yb versus Nb/Yb (Pearce 2008), **c** $SiO_2/50$–TiO_2–K_2O ternary (*FM* fractional crystallization of MORB; *AA* anatexis of amphibolite; *ADD* anatexis of diabase dikes; *AG* anatexis of gabbro [fields from France et al. 2010]; x: Troodos and Oman [from Grimes et al. 2013]) and **d** TiO_2 versus SiO_2 (Koepke et al. 2007) diagrams for the Ekecikdağ ophiolitic rocks

of the İzmir–Ankara–Erzincan ridge, inherited from an inverted ridge-transform configuration. Overall, there is an agreement that these dominantly crustal rocks were then obducted on the CACC metamorphic basement. Our interpretation on the gabbroic host of the plagiogranite is in agreement with the previous studies as the Ekecikdağ rocks belong to the SSZ-type Central Anatolian Ophiolites, which were overthrusted the CACC basement. The exception to this approach is Kadıoğlu et al. (1998, 2003) and Deniz and Kadıoğlu (2016), who excludes the Ekecikdağ gabbro from the Central Anatolian Ophiolites and considers it as a member of "gabbroic plutons." Their explanations based mainly on geochemical data, Ar–Ar ages from gabbros from the Ağaçören area (i.e., 78.0 ± 0.3 to 78.8 ± 1.0 Ma) and aeromagnetic anomalies suggesting gabbros in this area are intrusions coeval with Late Cretaceous calc-alkaline granitoids in Central Anatolia (e.g., Kadıoğlu et al. 2003). They interpret mafic rocks as derived from a metasomatized upper mantle source above a subduction zone, which were injected into felsic magma chambers producing coeval granitoid to gabbroic plutons, and extend their interpretations to further south by mapping the Ekecikdağ rocks as belong to this igneous association. However, Göncüoglu and Türeli (1993a, b), Türeli et al. (1993) and Köksal et al. (2012) described the gabbroic rocks in this region as roof pendants on granitic plutons and infer ophiolitic origin.

The plagiogranites as a member of the Central Anatolian Ophiolites are also a matter of debate. First, Göncüoglu and

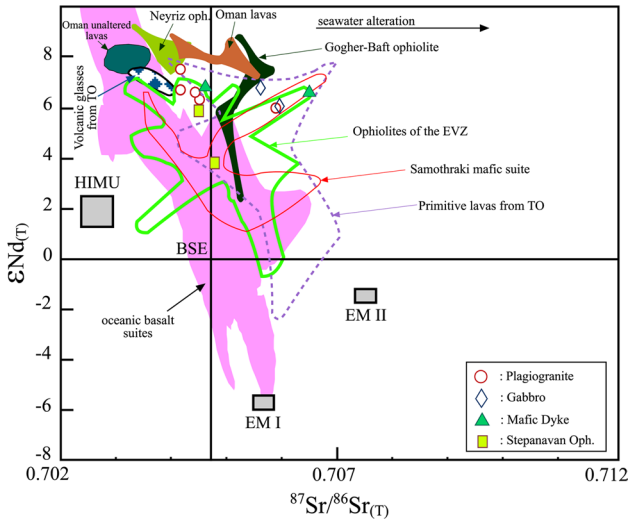

Fig. 13 $\varepsilon Nd_{(T)}$ versus $^{87}Sr/^{86}Sr_{(T)}$ diagram of the Ekecikdağ ophiolitic rocks. BSE (Bulk Silicate Earth) and oceanic basalt suites are from Zindler and Hart (1986); EM-I (enriched mantle-I), EM-II (enriched mantle-II) and HIMU (high μ mantle) are from Hofmann (2003). Other areas for comparison: primitive lavas from *TO* Troodos ophiolite (McCulloch and Cameron 1983), ophiolites of the *EVZ* Eastern Vardar Zone (Zachariadis 2007), Samothraki mafic suite (Koglini et al. 2009), volcanic glasses from *TO* Troodos ophiolite (Rautenschlein et al. 1985), Goghar-Baft ophiolite and Neyriz oph.—ophiolite (Shafaii Moghadam et al. 2013), Oman lavas and Oman unaltered lavas (Godard et al. 2006), Stepanavan Oph.—ophiolite (Rolland et al. 2009)

Türeli (1993a, b) suggested that the plagiogranites of the Ekecikdağ mafic body have been formed in a fore-arc setting by fractionation of basic magma during intra-oceanic subduction. Floyd et al. (1998) described the Sarıkaraman plagiogranite as formed in the roof of a dynamic and evolving gabbroic magma chamber mostly by fractional crystallization and partly by partial melting. From different parts of the CACC, Koçak et al. (2005, 2014) provided data from oceanic plagiogranites in relation with massive gabbros and mafic dykes. They also interpreted these units to be derived from a SSZ-type mantle origin. Consequently, there is more or less consensus on a SSZ tectonic environment for genesis of the plagiogranites in previous studies (e.g., Yalınız et al. 1999; Floyd et al. 1998, 2000; Koçak et al. 2005, 2014).

Our new geochemical data, on the other hand, imply that the Ekecikdağ plagiogranite is likely to be formed by partial melting of a depleted gabbro source. This is also supported by isotope data. From the same plagiogranite samples used in this study (i.e., EK-40 and EK-41), Grimes et al. (2013) presented oxygen isotopes of zircons along with those from different ophiolites of the world. Their findings from the Ekecikdağ samples reveal average $\delta^{18}O$ values of 4.8 ± 0.31 and 4.88 ± 0.39 ‰. According to Grimes et al. (2013), these oxygen isotope data below the average mantle value of 5.3 ‰ infer contamination by hydrothermally altered crust. This melting and/or contamination may be generated by crust altered to low-$\delta^{18}O$ values, which is likely to result from the effect of seawater-derived fluids (at temperatures more than 300 °C), a typical case in the base of the sheeted dike complex and in the upper gabbros (Grimes et al. 2013). As a result, our geochemical data including Nd–Sr–Pb isotopic characteristics together with oxygen isotope data of Grimes et al. (2013) infer partial melting of depleted mantle source which might have been further modified by a subduction component. Therefore, our findings support evolution of the Ekecikdağ plagiogranites through hydrous partial melting of gabbros rather than generation by fractional crystallization of a MORB source. Although plagiogranites, gabbros and mafic dykes in the study area reveal broadly similar chemical features, the field relations point to age differences. Therefore, gabbroic source, from which plagiogranites were originated, should be different and older than gabbros found in the study area. In addition mafic dykes should designate the latest igneous products in the study area. Further depiction of evolution stages of the ophiolites needs age data from gabbros and mafic dykes in the region.

Regarding the geological evolution of the Central Anatolian Ophiolites, previously published data suggest that the formation and emplacement of SSZ-type ophiolites in Central Turkey should have been realized in a short time interval, as they were at about 90–95 Ma, obducted on the CACC (e.g., Göncüoglu and Türeli 1993a; Floyd et al. 1998, 2000; Yalınız et al. 1996, 2000) and later intruded by collisional- to postcollisional-type Late Cretaceous granitoids (e.g., Yalınız et al. 1999; Köksal et al. 2012, 2013). The U–Pb age of the Sarıkaraman plagiogranite (i.e., $^{206}Pb/^{238}U$ age of 90.56 ± 0.14 Ma; van Hinsbergen et al. 2016) also confirms this phenomenon since the collisional granitoids in the CACC, which were formed by crustal thickening after obduction of ophiolites, reveal an age of 85–75 Ma (e.g., Toksoy-Köksal et al. 2009b; Köksal et al. 2012). The Ekecikdağ plagiogranites and the Sarıkaraman plagiogranites being in the same tectonic setting and reveal similar chemistry (e.g., Figs. 7, 10, 12) are assumed to be concurrent. Typical contemporary examples of plagiogranites from SSZ fore-arc ophiolitic suits (e.g., Metcalf and Shervais 2008) are found in Troodos (e.g., 91.6 ± 1.4 Ma, Mukasa and Ludden 1987) and in Oman (ca. 95 Ma, Tilton et al. 1981).

Considering our new data and the state-of-the-art knowledge on the regional geological constraints, a new scenario is suggested (Fig. 16). The model cogitates that the İzmir–Ankara-Erzincan Ocean was the main Neotethyan oceanic

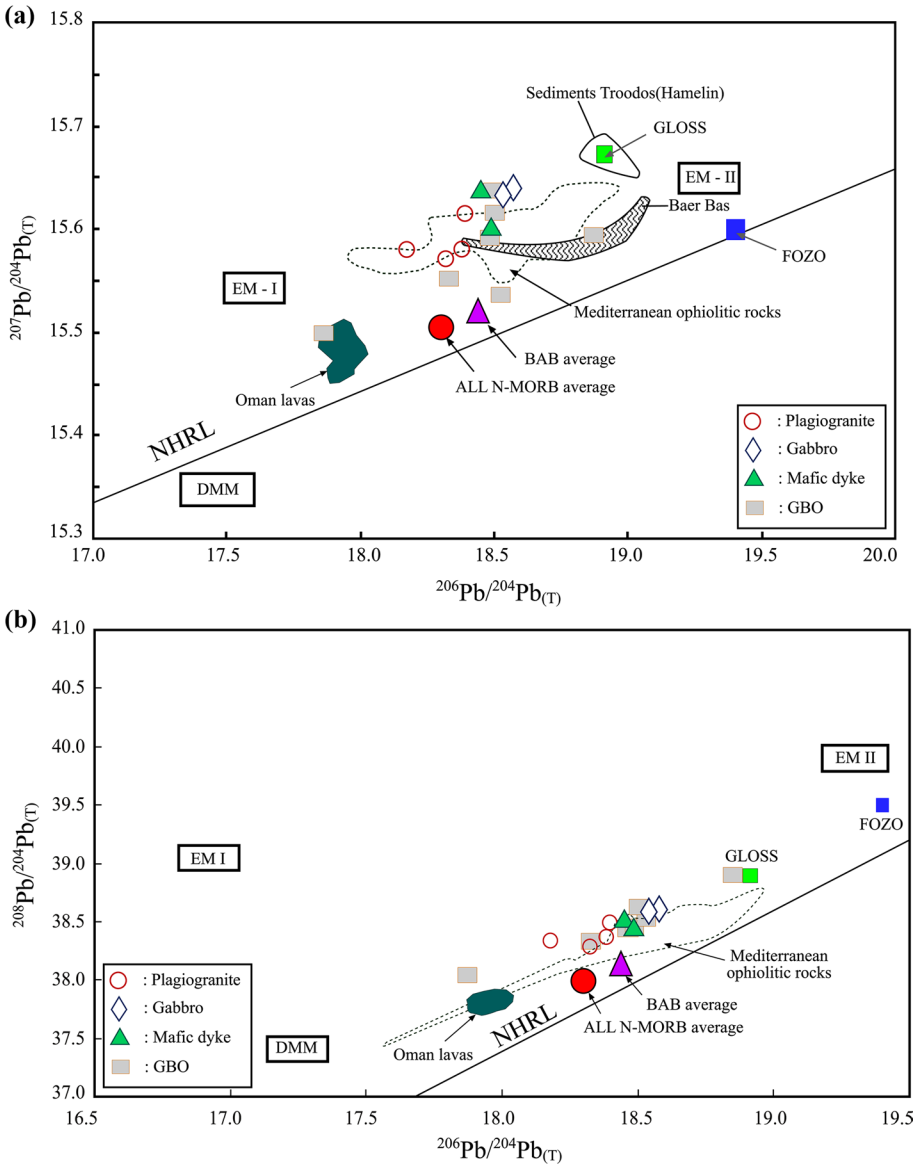

Fig. 14 **a** $^{207}Pb/^{204}Pb_{(T)}$ versus $^{206}Pb/^{204}Pb_{(T)}$ **b** $^{208}Pb/^{204}Pb_{(T)}$ versus $^{206}Pb/^{204}Pb_{(T)}$ diagrams for the Ekecikdağ ophiolitic rocks. All N-MORB average and BAB (back-arc basin) average are from Gale et al. (2013), EM-I (enriched mantle-I), EM-II (enriched mantle-II) and DMM (depleted MORB mantle) are from Hofmann (2003), NHRL (Northern Hemisphere Reference Line), GLOSS [globally subducting sediments] and FOZO [focal zone] are from Workman et al. (2004), Troodos sediments are from Hamelin et al. (1988), Troodos ophiolitic rocks are from Hamelin et al. (1984, 1988); Rautenschlein et al. (1985); Booij et al. (2000), and Baer Bas (Baer Bassit ophiolite) field is from Hamelin et al. (1984), GBO [Gogher-Baft ophiolite] is from Shafaii Moghadam et al. (2013), Oman lavas are from Godard et al. (2006)

branch between the Gondwana-derived Tauride-Anatolide continent and the Cimmerian Sakarya Composite Terrane (sensu Göncüoglu et al. 1997) since the Early Mesozoic. More than one intra-oceanic subduction was generated along different segments of this ocean since Mid-Jurassic (e.g., Çelik et al. 2011). The SSZ-type İAEO belt ophiolites were derived from one of these intra-oceanic subductions in an arc basin setting by partial melting of the oceanic crust (Fig. 16a, b) at about 90 my. Although it is difficult to describe the Ekecikdağ ophiolitic rocks as belong to back-arc or fore-arc oceanic environments geochemically (e.g., Fig. 9), short time interval between generation and obduction (i.e., ca. 5 Ma) infers a fore-arc setting. Moreover, their higher initial Pb isotope ratios with respect to back-arc basin average data besides N-MORB average data (Gale et al. 2013) are likely to rule out the back-arc basin origin. The newly formed SSZ-type ophiolite obducted onto the Tauride-Anatolide continental crust, already metamorphosed to represent basement units of the CACC (Fig. 16c) at about 85 my. The obduction resulted in melting of the CACC crust to produce the mainly S-type Central Anatolian Granitoids (e.g., Yalınız et al. 1999, 2000; Köksal et al. 2012, 2013). The ongoing convergence between the CACC crust and Sakarya Terranes continental crust with its marginal arc produced a huge mélange complex (Fig. 16d), the Ankara Mélange, including numerous blocks representing the MORB, OIB and SSZ-type ophiolitic blocks that range from Late Triassic to Campanian in age (e.g., Bortoletti

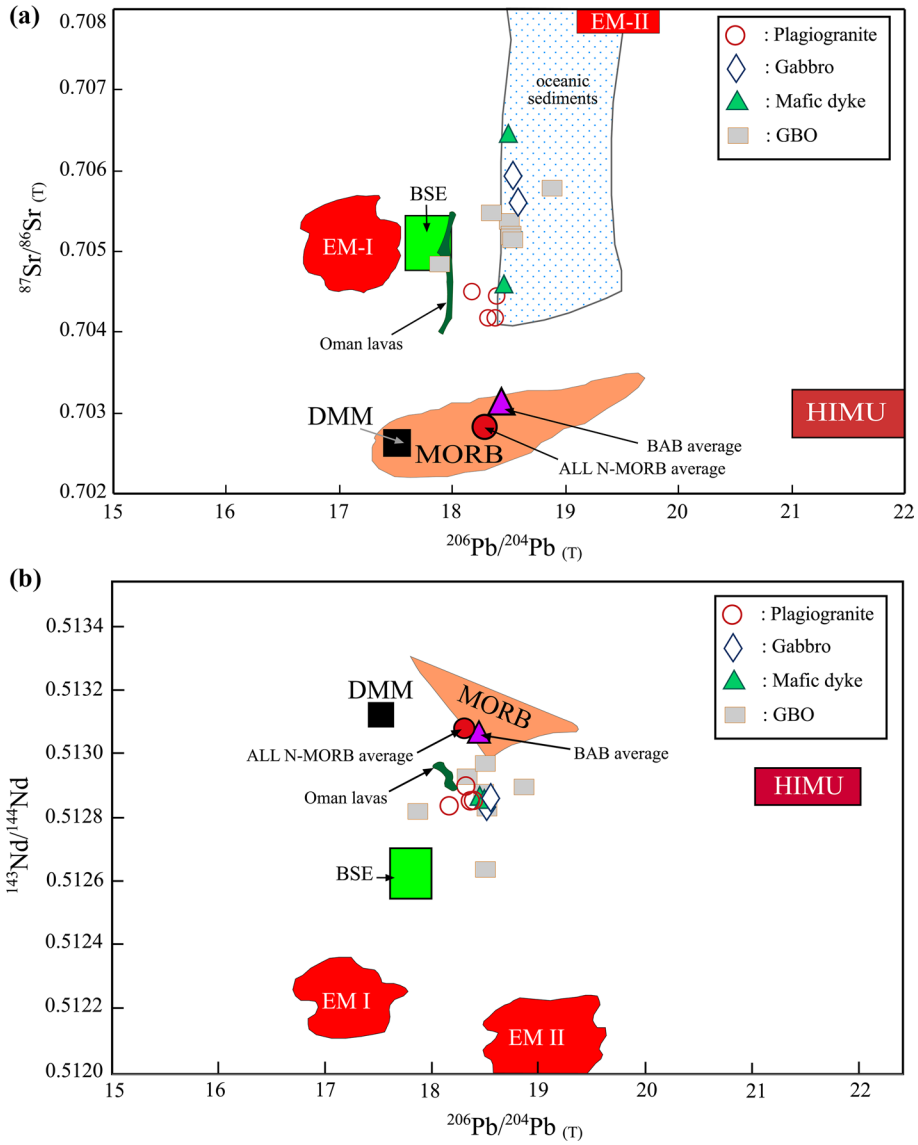

Fig. 15 **a** $^{87}Sr/^{86}Sr_{(T)}$ versus $^{206}Pb/^{204}Pb_{(T)}$ **b** $^{143}Nd/^{144}Nd_{(T)}$ versus $^{206}Pb/^{204}Pb_{(T)}$ diagrams for the Ekecikdağ ophiolitic rocks (field of oceanic sediments, EM-I, EM-II, BSE, MORB and HIMU are from Zindler and Hart (1986); all N-MORB average and BAB average are from Gale et al. (2013); DMM is from Workman and Hart (2005)), GBO (Gogher-Baft ophiolite) is from Shafaii Moghadam et al. (2013), and Oman lavas are from Godard et al. (2006)

et al. 2013). The İAEO belt ophiolites were intruded at about 75 my by monzonitic granitoids, which were derived by postobductional relaxation of the CACC crust and related asthenospheric uplifting (e.g., Köksal et al. 2004, 2013).

Similar processes with the Late Cretaceous SSZ-type ophiolitic sequences are known on the Eastern continuation of Neotethys in Eastern Turkey, Armenia and Iran (e.g., Rolland et al. 2009; Hässig et al. 2013). Upper Cretaceous calc-alkaline lavas from the Stepanavan area (Armenia), which show similar isotopic characteristics with Ekecikdağ ophiolitic rocks, were interpreted to belong to volcanic arc series linked to the subduction of the Neotethys Ocean preceding the obduction of the ophiolitic rocks onto the South Armenian Block (Rolland et al. 2009). Besides, Gogher-Baft, Neyriz and Dehshir ophiolites from Iran, revealing similar isotope characteristics with Ekecikdağ ophiolitic rocks, were described as SSZ ophiolites with lesser MORB-type lavas and characterize subduction initiation (Shafaii Moghadam et al. 2013).

Conclusions

The Late Cretaceous Ekecikdağ plagiogranites occur as dykes and small stocks within the Ekecikdağ gabbro that belongs to the allochthonous members of the İAEO belt. The gabbros and the plagiogranites are cut by mafic dykes. Geochemically, the plagiogranites and their gabbroic host are described by their high LILE/HFSE ratios with

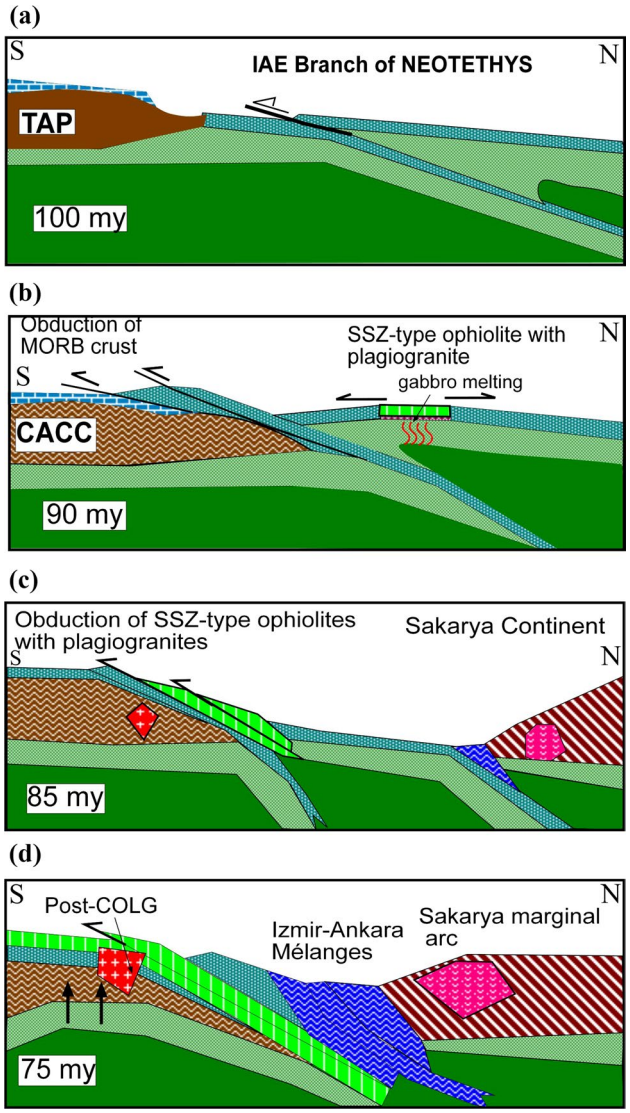

Fig. 16 Geodynamic scenario for the evolution of the Central Anatolian plagiogranitic rocks within the closing İzmir–Ankara–Erzincan Oceanic Branch of Neotethys (modified after Yalınız et al. 2000). The details are given in the text. Abbreviations: TAP: Tauride-Anatolide Platform, CACC: Central Anatolian Crystalline Complex

depletion in Nb, Ti and LREE with respect to N-MORB. These geochemical features, including Nd–Sr–Pb isotopic characteristics, are similar to the Late Cretaceous SSZ-type ophiolitic rocks from Troodos, Oman, Greece, Armenia and Iran. Geochemical data including radiogenic isotopes suggest that the plagiogranites were formed by partial melting of a depleted gabbro source in a fore-arc setting by involvement of a subduction component rather than generation by fractional crystallization of a MORB source. The chemical composition of the mafic dykes is in accordance with the SSZ character of the Ekecikdağ gabbro.

Acknowledgments Authors thank Radiogenic Isotope Laboratory of Middle East Technical University—Central Laboratory, for Sr–Nd–Pb isotope analyses. S. Köksal thanks to Prof. Dr. Rolf L. Romer for his supervision in the isotope ratio methods, Dr. Selin Süer and Sultan Atalay for their assistance during the clean laboratory facilities and Remzi Saraçoğlu for technical support. An anonymous reviewer, guest editor and Dr. Semih Gürsu are acknowledged for their constructive reviews and comments, which significantly helped to modify the manuscript. Authors thank to IGCP 589 Project leader Prof. Dr. Jin Xiaochi for encouraging us to contribute the special volume "Asian Tethyan Realm."

References

Aldiss DT (1981) Plagiogranites from the ocean crust and ophiolites. Nature 289:577–578

Arth JG (1979) Some trace elements in trondhjemites—their implications to magma genesis and paleotectonic setting. In: Barker F (ed) Trondhjemite, dacites and related rocks. Elsevier, New York, pp 123–132

Barbieri M, Caggianelli A, Di Florio MR, Lorenzoni S (1994) Plagiogranites and gabbroic rocks from the Mingora ophiolitic mélange, Swat Valley, NW Frontier Province, Pakistan. Miner Mag 58:553–566

Barker F (1979) Trondhjemite: definition, environment, and hypotheses of origin. In: Barker F (ed) Trondhjemite, dacites and related rocks. Elsevier, New York, pp 1–12

Bonev N, Stampfli G (2009) Gabbro, plagiogranites and associated dykes in the supra-subduction zone Evros Ophiolites, NE Greece. Geol Mag 146(1):72–91

Booij E, Bettison-Varga L, Farthing D, Staudigel H (2000) Pb-isotope systematics of a fossil hydrothermal system from the troodos ophiolite, cyprus: evidence for a polyphased alteration history. Geochim Cosmochim Acta 64:3559–3569

Bortolotti V, Chiari M, Göncüoglu MC, Marcucci M, Principi G, Tekin UK, Saccani E, Tassinari R (2013) Age and geochemistry of basalt-chert associations in the ophiolites of the İzmir–Ankara mélange east of Ankara, Turkey: preliminary data. Ofioliti 38(2):157–173

Bozkurt E, Mittwede S (2001) Introduction to the geology of Turkey—a synthesis. Int Geol Rev 43:578–594

Brophy JG, Pu X (2012) Rare earth-SiO_2 systematics of mid-ocean ridge plagiogranites and host gabbros from the Fournier oceanic fragment, New Brunswick, Canada: a field evaluation of some model predictions. Contrib Miner Petrol 164:191–204. doi:10.1007/s00410-012-0732-x

Çelik ÖF, Marzoli A, Marschik R, Chiaradia M, Neubauer F, Öz İ (2011) Early-middle Jurassic intra-oceanic subduction in the İzmir–Ankara–Erzincan Ocean, Northern Turkey. Tectonophysics 509:120–134

Chauvel C, Blichert-Toft J (2001) A hafnium isotope and trace element perspective on melting of the depleted mantle. Earth Planet Sci Lett 190:137–151

Coish RA, Hickey R, Frety FA (1983) Rare earth element geochemistry of the Betts Cove ophiolite, Newfoundland: complexities in ophiolite formation. Geochim Cosmochim Acta 46:2117–2134

Coleman RG, Donato MM (1979) Oceanic plagiogranite revisited. In: Barker F (ed) Trondhjemite, dacites and related rocks. Elsevier, New York, pp 149–167

Coleman RG, Peterman ZE (1975) Oceanic plagiogranite. J Geophys Res 80:1099–1108

Deniz K, Kadıoğlu YK (2016) Assimilation and fractional crystallization of foid-bearing alkaline rocks: Buzlukdağ intrusives, Central Anatolia, Turkey. Turk J Earth Sci 25(4):341–366

Dupré B, Allègre CJ (1980) Pb–Sr–Nd isotopic correlation and the chemistry of the North Atlantic mantle. Nature 286:17–22
Erdoğan B, Akay E, Uğur MS (1996) Geology of the Yozgat region and evolution of the collisional Çankırı Basin. Int Geol Rev 38(9):788–806
Fedo CM, Nesbitt HW, Young GM (1995) Unraveling the effects of potassium metasomatism in sedimentary rocks and paleosols, with implications for paleoweathering conditions and provenance. Geology 23:921–924
Floyd PA, Yalınız MK, Göncüoglu MC (1998) Geochemistry and petrogenesis of intrusive and extrusive ophiolitic plagiogranites, Central Anatolian Crystalline Complex, Turkey. Lithos 42:225–241
Floyd PA, Göncüoglu MC, Winchester JA, Yalınız MK (2000) Geochemical character and tectonic environment of Neotethyan ophiolitic fragments and metabasites in the Central Anatolian Crystalline Complex, Turkey. In: Bozkurt E, Winchester JA, Piper JDA (ed) Tectonics and magmatism in Turkey and the surrounding area. Geological Society of London, Special Publication, 173:183–202
France L, Koepke J, Ildefonse B, Cichy S, Deschamps F (2010) Hydrous partial melting in the sheeted dike complex at fast spreading ridges: experimental and natural observations. Contrib Miner Petrol 160:683–704
Gale A, Dalton CA, Langmuir CH, Su Y, Schilling J-G (2013) The mean composition of ocean ridge basalts. Geochem Geophys Geosyst 14(3):489–518. doi:10.1029/2012GC004334
Godard M, Bosch D, Einaudi F (2006) A MORB source for low-Ti magmatism in the Semail ophiolite. Chem Geol 234:58–78
Göncüoglu MC (2014) Comments on a single versus multi-armed Southern Neotethys in SE Turkey and Iran. IGCP589 Development of the Asian Tethyan realm: Genesis, process and outcome. Abstracts and Proceedings, 89–95
Göncüoglu MC, Türeli K (1993a) Petrology and geodynamic interpretation of plagiogranites from Central Anatolian Ophiolites (Aksaray-Turkey). Turk J Earth Sci 2:195–203
Göncüoglu MC, Türeli TK (1993b) Petrology and geodynamic interpretation of plagiogranites from Central Anatolian ophiolites (Aksaray, Turkey). Ofioliti 18(2):187
Göncüoglu MC, Toprak GMV, Kuşçu I, Erler A, Olgun E (1991) Geology of the western part of the Central Anatolian Massif: part I southern part, (Report No: 2909), Turkish Petroleum Company
Göncüoglu MC, Dirik K, Kozlu H (1997) Pre-Alpine and Alpine Terranes in Turkey: explanatory notes to the terrane map of Turkey. Ann Geol Pays Hell 37:515–536
Göncüoglu MC, Sayıt K, Tekin UK (2010) Oceanization of the northern Neotethys: geochemical evidence from ophiolitic melange basalts within the İzmir–Ankara suture belt, NW Turkey. Lithos 116:175–187
Göncüoglu MC, Tekin UK, Sayıt K, Bedi Y, Uzunçimen-Keçeli S (2015) Evolution of the Neotethyan branches in the Eastern Mediterranean: petrology and ages of oceanic basalts. Igcp589 the fourth symposium of the international geosciences programme abstracts and proceedings, 17–19
Grimes CB, Ushikubo T, Kozdon R, Valley JW (2013) Perspectives on the origin of plagiogranites in ophiolites from oxygen isotopes in zircon. Lithos 179:48–66
Hamelin B, Dupré B, Allègre CJ (1984) The lead isotope systematics of ophiolite complexes. Earth Planet Sci Lett 67:351–366
Hamelin B, Dupré B, Brévart O, Allègre CJ (1988) Metallogenesis at paleo-spreading centers: lead isotopes in sulfides, rocks and sediments from the Troodos ophiolite (Cyprus). Chem Geol 68:229–238
Hässig M, Rolland Y, Sosson M, Galoyan G, Sahakyan L, Topuz G, Çelik ÖF, Avagyan A, Müller C (2013) Linking the NE Anatolian and Lesser Caucasus ophiolites: evidence for large-scale obduction of oceanic crust and implications for the formation of the Lesser Caucasus-Pontides Arc. Geodin Acta 26(3–4):311–330
Hatzipanagiotou K, Tsikouras B (1999) Plagiogranites in the Hellenic ophiolites. Ofioliti 24:283–292
Hoernle K (1998) Geochemistry of Jurassic oceanic crust beneath Gran Canaria (Canary Islands): implications for crustal recycling and assimilation. J Petrol 39:859–880
Hofmann AW (2003) Sampling mantle heterogeneity trough oceanic basalts: isotopes and trace elements. In: Carlson RW, Holland HD, Turekian KK (eds) Treatise on geochemistry, vol 2., The mantle and coreElsevier, Oxford, pp 61–101
Hollocher K, Robinson P, Walsh E, Roberts D (2012) Geochemistry of amphibolite-facies volcanics and gabbros of the Støren nappe in extensions West and Southwest of Trondheim, western gneiss region, Norway: a key to correlations and paleotectonic settings. Am J Sci 312:357–416. doi:10.2475/04.2012.01
Hughes CJ (1973) Spilites, keratophyres and the igneous spectrum. Geol Mag 109:513–527
İlbeyli N (1993) Petrography and petrology of the ultramafic-mafic rocks of the Felahiye (Kayseri) region: Unpubl. M.Sc. thesis, University of Ankara, Turkey (in Turkish)
Irvine TN, Baragar WRA (1971) A guide to the geochemical classification of the common volcanic rocks. Can J Earth Sci 8:523–548
Jafri SH, Charan SN, Govil PK (1995) Plagiogranite from the Andaman ophiolite belt, Bay of Bengal, India. J Geol Soc Lond 152:681–687
Kadıoğlu YK, Ates A, Güleç N (1998) Structural interpretation of gabbroic rocks in Ağaçören Granitoid, Central Turkey: field observations and aeromagnetic data. Geol Mag 135(02):245–254
Kadıoğlu YK, Dilek Y, Güleç N, Foland KA (2003) Tectonomagmatic evolution of bimodal plutons in the Central Anatolian Crystalline Complex, Turkey. J Geol 111(6):671–690
Kılıç AD (2009) Petrographical and geochemical properties of plagiogranites and gabbros in Guleman ophiolite. Miner Res Exp Bull 139:33–49
Koçak K, Işık F, Arslan M, Zedef V (2005) Petrological and source region characteristics of ophiolitic hornblende gabbros from the Aksaray and Kayseri regions, Central Anatolian Crystalline Complex, Turkey. J Asian Earth Sci 25:883–891
Koçak K, Leake BE, Söğüt R (2014) Geochemical characteristics of oceanic plagiogranite and basic dikes at the sheeted dike complex of Central Anatolian Ophiolites at Bozkır (Ortakoy-Aksaray/TURKEY) Dam. Latest trends in energy, environment and development, proceedings of the 7th international conference on environmental and geological science and engineering, p. 296–299
Koepke J, Berndt J, Feig ST, Holtz F (2007) The formation of SiO_2-rich melts within deep oceanic crust by hydrous partial melting of gabbros. Contrib Miner Petrol 153:67–84
Koglini N, Kostopoulos D, Reischmann T (2009) Geochemistry, petrogenesis and tectonic setting of the Samothraki mafic suite, NE Greece: trace-element, isotopic and zircon age constraints. Tectonophysics 473:53–68
Köksal S, Romer RL, Göncüoglu MC, Toksoy-Köksal F (2004) Timing of the transition from the post-collisional to A-type magmatism: titanite U/Pb ages from the alpine Central Anatolian Granitoids, Turkey. Int J Earth Sci 93:974–989
Köksal S, Göncüoglu MC, Toksoy-Köksal F (2010) Re-evaluation of the petrological features of the Ekecikdağ Plagiogranites in Central Anatolia/Turkey. Symposium of Geological Society of America, Tectonic Crossroads: evolving orogens of Eurasia-Africa-Arabia, Ankara, Turkey, Abstracts, p. 83
Köksal S, Möller A, Göncüoglu MC, Frei D, Gerdes A (2012) Crustal homogenization revealed by U-Pb zircon ages and Hf isotope evidence from the Late Cretaceous granitoids of the Agaçören

intrusive suite (Central Anatolia/Turkey). Contrib Miner Petrol 163:725–743. doi:10.1007/s00410-011-0696-2

Köksal S, Toksoy-Köksal F, Göncüoglu MC, Möller A, Gerdes A, Frei D (2013) Crustal source of the Late Cretaceous Satansari monzonite (Central Anatolia/Turkey) and its significance for the Alpine geodynamic evolution. J Geodyn 65:82–93. doi:10.1016/j.jog.2012.06.003

Kuroda PK, Sandell EB (1954) Geochemistry of molybdenum. Geochim Cosmochim Acta 6(1):35–63

Large RR, Gemmell JB, Paulick H, Huston DL (2001) The alteration box plot: a simple approach to understanding the relationship between alteration mineralogy and lithochemistry associated with volcanic-hosted massive sulfide deposits. Econ Geol 96:957–971

Magganas A (2007) Plagiogranitic rocks of Evros Ophiolite, NE Greece. Bull Geol Soc Greece 40:884–898

McCulloch MT, Cameron WE (1983) Nd-Sr isotopic study of primitive lavas from the troodos ophiolite, cyprus: evidence for a subduction-related setting. Geology 11:727–731

Metcalf RV, Shervais JW (2008) Suprasubduction-zone ophiolites: is there really an ophiolite conundrum? In: Wright JE, Shervais JW (ed) Ophiolites, arcs, and batholiths: a tribute to Cliff Hopson, Geological Society of America Special Paper 438:191–222. doi:10.1130/2008.2438(07)

Mirza TA, Ismail SA (2007) Origin of plagiogranites in the Mawat ophiolite complex, Kurdistan region, NE Iraq. J Kirkuk Univ Sci Stud 2(1):1–20

Moix P, Beccaletto L, Kozur HW, Hochard C, Rosselet F, Stampfli GM (2008) A new classification of the Turkish terranes and sutures and its implication for the Paleotectonic history of the region. Tectonophysics 451:7–39

Mukasa SB, Ludden JN (1987) Uranium-lead isotopic ages of plagiogranites from the Troodos ophiolite, Cyprus, and their tectonic significance. Geology 15:825–828

Okay Aİ, Tüysüz O (1999) Tethyan sutures of northern Turkey. In: Durand B, Jolivet L, Horwarth E, Seranne M (ed) The Mediterranean Basins: tertiary extension within the Alpine Orogen. Geological Society, London, Special Publications, 156:475–515

Pearce JA (1983) Role of the sub-continental lithosphere in magma genesis at active continental margins. In: Hawkesworth CJ, Norry MJ (eds) Continental basalts and mantle xenoliths. Shiva Publishing Ltd., Cambridge, pp 230–249

Pearce JA (2008) Geochemical fingerprinting of oceanic basalts with applications to ophiolite classification and the search for Archean oceanic crust. Lithos 100:14–48

Pearce JA, Harris NBW, Tindle AGW (1984a) Trace element discrimination diagrams for the tectonic interpretation of granitic rocks. J Petrol 25:956–983

Pearce JA, Lippard SJ, Roberts S (1984b) Characteristics and tectonic significance of supra-subduction zone ophiolites. Geol Soc Lond Spec Publ 16:77–94

Rautenschlein M, Jenner GA, Hertogen J, Hofmann AW, Kerrich R, Schmincke H-U, White WM (1985) Isotopic and trace element composition of volcanic glasses from the Akaki Canyon, Cyprus: implications for the origin of the Troodos ophiolite. Earth Planet Sci Lett 75:369–383

Rolland Y, Galoyan G, Bosch D, Sosson M, Corsini M, Fornari M, Verati C (2009) Jurassic back-arc and Cretaceous hot-spot series in the Armenian ophiolites—implications for the obduction process. Lithos 112:163–187

Romer RL, Forster H-J, Breitkreuz C (2001) Intracontinental extensional magmatism with a subduction fingerprint: the late Carboniferous Halle Volcanic Complex (Germany). Contrib Miner Petrol 141:201–221

Ruks TW, Piercey SJ, Ryan JJ, Villeneuve ME, Creaser RA (2006) Mid- to Late Paleozoic K-Feldspar Augen granitoids of the Yukon-Tanana Terrane, Yukon, Canada: implications for crustal growth and tectonic evolution of the Northern Cordillera. Geol Soc Am Bull 18:1212–1231

Shafaii Moghadam H, Stern RJ, Kimura J-I, Hirahara Y, Senda R, Miyazaki T (2012) Hf–Nd isotope constraints on the origin of Dehshir ophiolite, Central Iran. Isl Arc 21:202–214

Shafaii Moghadam H, Stern RJ, Chiaradia M, Rahgoshav M (2013) Geochemistry and tectonic evolution of the Late Cretaceous Gogher-Baft ophiolite, Central Iran. Lithos 168–169:33–47

Spitz G, Darling R (1978) Major and minor element lithogeochemical anomalies surrounding the Louvem copper deposit, Val d'Or, Quebec. Can J Earth Sci 15:1161–1169

Sun S-S, McDonough WF (1989) Chemical and isotopic systematics of oceanic basalts; implications for mantle composition and processes. In: Saunders AD, Norry MJ (ed) Magmatism in the Ocean Basins. Geological Society of London, Special Publications, pp 313–345

Tekin UK, Göncüoglu MC, Uzunçimen S (2012) Radiolarian assemblages of Middle and Late Jurassic to Early Late Cretaceous (Cenomanian) ages from an olistolith record pelagic deposition within the Bornova Flysch Zone in western Turkey. Bull Soc Géol Fr 183(4):307–318

Tilton GR, Hopson CA, Wright JG (1981) Uranium-lead isotopic ages of the Samail ophiolite with applications to Tethyan ocean ridge tectonics. J Geophys Res 86:2763–2775

Toksoy-Köksal F, Göncüoglu MC, Yalınız MK (2001) Petrology of the Kurançalı phlogopite metagabbro: an island arc-type ophiolitic sliver in the Central Anatolian Crystalline Complex. Int Geol Rev 43:624–639

Toksoy-Köksal F, Oberhaensli R, Göncüoglu MC (2009a) Hydrous aluminosilicate metasomatism in an intra-oceanic subduction zone: implications from the Kurançalı (Turkey) ultramafic-mafic cumulates within the Alpine Neotethys Ocean. Miner Petrol 95:273–290. doi:10.1007/s00710-009-0044-7

Toksoy-Köksal F, Gerdes A, Göncüoglu MC, Möller A, Frei D, Köksal S (2009b) U-Pb age and isotope data from the S- and I-type syn-collisional granites in Ekecikdağ area, Central Anatolia. Geochimica et Cosmochmica Acta, 73, Supplement, Goldschmidt Conference Abstracts A1335

Toksoy-Köksal F, Köksal S, Göncüoglu MC (2010) Is a single model adequate to explain origin of the gabbros from Central Anatolia, Turkey? Symposium of Geological Society of America, Tectonic Crossroads: evolving orogens of Eurasia-Africa-Arabia, Ankara, Turkey, Abstracts, p 83

Türeli TK, Göncüoglu MC, Akıman O (1993) Origin and petrology of Ekecikdağ Granitoid in western Central Anatolian Massif. Miner Res Exp Bull 115:15–28

van Hinsbergen DJJ, Maffione M, Plunder A, Kaymakçı N, Ganerød M, Hendriks BWH, Corfu F, Gürer D, de Gelder GINO, Peters K, McPhee PJ, Brouwer FM, Advokaat EL, Vissers RLM (2016) Tectonic evolution and paleogeography of the Kırşehir Block and the Central Anatolian Ophiolites, Turkey. Tectonics 35(4):983–1014. doi:10.1002/2015TC004018

Weiss D, Kieffer B, Maerschalk C, Barling J, de Jong J, Williams GA, Hanano D, Preorius W, Mattielli N, Scoates JS, Goolaerts A, Friedman M, Mahoney JB (2006) High-precision isotopic characterization of USGS reference materials by TIMS and MC–ICP–MS. Geochem Geophys Geosyst 7(8):Q08006. doi:10.1029/2006GC001283

Winchester JA, Floyd PA (1977) Geochemical discrimination of different magma series and their different products using immobile elements. Chem Geol 20:325–343

Workman RK, Hart SR (2005) Major and trace element composition of the depleted MORB mantle (DMM). Earth Planet Sci Lett 231:53–72

Workman RK, Hart SR, Jackson M, Regelous M, Farley KA, Blusztajn J, Kurz M, Staudigel H (2004) Recycled metasomatized lithosphere as the origin of the Enriched Mantle II (EM2) end-member: evidence from the Samoan Volcanic Chain. Geochem Geophys Geosyst 5:Q04008. doi:10.1029/2003GC000623

Yalınız MK, Floyd PA, Göncüoglu MC (1996) Supra-subduction zone ophiolites of Central Anatolia, geochemical evidence from the Sarikaraman ophiolite, Aksaray, Turkey. Miner Mag 60:697–710

Yalınız MK, Aydın NS, Göncüoglu MC, Parlak O (1999) Terlemez quartz monzonite of Central Anatolia (Aksaray-Sarıkaraman): age, petrogenesis and geotectonic implications for ophiolite emplacement. Geol J 34:233–242

Yalınız MK, Floyd PA, Göncüoglu MC (2000) Geochemistry of volcanic rocks from the Çiçekdag ophiolite, Central Anatolia, Turkey, and their inferred tectonic setting within the northern branch of the Neotethyan ocean. In: Bozkurt E, Winchester JA, Piper JDA (ed) Tectonics and magmatism in Turkey and the surrounding area, Geological Society of London, Special Publications, 173:203–218

Zachariadis PT (2007) Ophiolites of the eastern Vardar Zone, N. Greece. Dissertationi Institut für Geowissenschaften, Johannes Gutenberg Universität, Mainz, Germany, p 221

Zindler A, Hart SR (1986) Chemical Geodynamics. Annu Rev Earth Planet Sci 14:493–571